

# ECOLOGY LETTERS

## Microbial symbionts buffer hosts from the demographic costs of environmental stochasticity

Journal:	<i>Ecology Letters</i>
Manuscript ID	ELE-01100-2023
Manuscript Type:	Letter
Date Submitted by the Author:	01-Nov-2023
Complete List of Authors:	Fowler, Joshua; University of Miami, Department of Biology; Rice University, Ecology and Evolutionary Biology Ziegler, Shaun; University of New Mexico, Department of Biology Whitney, Kenneth; University of New Mexico, Department of Biology Rudgers, Jennifer; University of New Mexico, Department of Biology Miller, Tom; Rice University, Ecology and Evolutionary Biology
Key Words:	symbiosis, stochasticity, demography, mutualism, Epichloë

SCHOLARONE™  
Manuscripts

# Microbial symbionts buffer hosts from the demographic costs of environmental stochasticity

Joshua C. Fowler<sup>1,2\*</sup>, Shaun Ziegler<sup>3</sup>, Kenneth D. Whitney<sup>3</sup>,  
Jennifer A. Rudgers<sup>3</sup>, Tom E.X. Miller<sup>1</sup>

<sup>1</sup>\*Department of BioSciences, Rice University, Houston, 77005, TX, USA.

<sup>2</sup>Department of Biology, University of Miami, Miami, 33146, FL, USA.

<sup>3</sup>Department of Biology, University of New Mexico, Albuquerque, 87131, NM, USA.

\*Corresponding author(s). E-mail(s): [jcf221@miami.edu](mailto:jcf221@miami.edu);

Contributing authors: [shaun.ziegler@gmail.com](mailto:shaun.ziegler@gmail.com); [whitneyk@unm.edu](mailto:whitneyk@unm.edu);

[jrudgers@unm.edu](mailto:jrudgers@unm.edu); [tom.miller@rice.edu](mailto:tom.miller@rice.edu);

Phone: 719-359-2960

## Author Contributions

J.C.F. contributed to data collection, data analysis, and led manuscript drafting. S.Z. contributed to data collection and manuscript revisions. K.D.W. contributed to research conception, data collection, and manuscript revisions. J.A.R. established transplant plots, contributed to research conception, data collection, and manuscript revisions. T.E.X.M. contributed to research conception, data collection, data analysis, and manuscript revisions.

## Data and Code Accessibility

Data will be made accessible as an Environmental Data Initiative package online  
**DOI:** [updated here when available](#). Code for all analysis is available through  
<https://github.com/joshuacfowler/Grass-Endophyte-Stochastic-Demography>

**Article Type:** Letter

**Running Title:** Symbiont-mediated demographic buffering

**Keywords:** stochasticity, demography, symbiosis, mutualism, Epichloë

**This file contains:** Abstract ( 150 words), Main Text (5397 words), Figures (1-4); Supporting Information - Supplemental Methods, Supplemental Figures A1-A28, Supplemental Tables S1-S3, References (66)

Manuscript submitted following PNAS style guidelines and can be reformatted upon revision

1  
2  
3  
4  
5  
6  
7  
8  
9  
10  
11  
12  
13  
14  
15  
16  
17  
18  
19  
20  
21  
22  
23  
24  
25  
26  
27  
28  
29  
30  
31  
32  
33  
34  
35  
36  
37  
38  
39  
40  
41  
42  
43  
44  
45  
46  
47  
48  
49  
50  
51  
52  
53  
54  
55  
56  
57  
58  
59  
60  
047  
048  
049  
050  
051  
052  
053  
054  
055  
056  
057  
058  
059  
060  
061  
062  
063  
064  
065  
066  
067  
068  
069  
070  
071  
072  
073  
074  
075  
076  
077  
078  
079  
080  
081  
082  
083  
084  
085  
086  
087  
088  
089  
090  
091  
092**Abstract**

Species' persistence in increasingly variable climates will depend on resilience against the fitness costs of environmental stochasticity. Most organisms host microbiota that shield against stressors. Here, we test the hypothesis that, by limiting exposure to environmental extremes, microbial symbionts reduce hosts' demographic variance. We parameterized stochastic models using data from a 14-year symbiont-removal experiment including seven grass species that host *Epichloë* fungal endophytes. Endophytes reduced variance in fitness by > 10%, on average. Hosts with "fast" life history traits that lacked longevity as an intrinsic buffer benefited most from symbiont-mediated variance buffering. Under current climate conditions, contributions of variance buffering were modest compared to symbiont benefits to mean fitness. However, simulations of increased stochasticity amplified benefits of variance buffering and made it the more important pathway of host-symbiont mutualism than elevated mean fitness. Microbial-mediated variance buffering is likely an important, yet cryptic, mechanism of resilience in an increasingly variable world.

For Review Only

## Introduction

Global climate change involves increases in environmental variability, including changes to precipitation patterns and the frequency of extreme weather events [1, 2]. Yet, the ecological consequences of increased variability are less well understood than those of changing climate means, such as long-term warming or drying. Incorporating environmental variability into forecasts of population dynamics can improve predictions of the future.

Classic theory predicts that long-term population growth rates (equivalently, population mean fitness) will decline under increased environmental stochasticity because the costs of bad years outweigh the benefits of good years – a consequence of nonlinear averaging [3, 4]. For example, in unstructured populations, the long-term stochastic growth rate in a fluctuating environment ( $\lambda_s$ ) will always be lower than the average growth rate ( $\bar{\lambda}$ ) by an amount proportional to the environmental variance ( $\sigma^2$ ):

$$\log(\lambda_s) \approx \log(\bar{\lambda}) - \frac{\sigma^2}{2\bar{\lambda}} \quad \text{Fig. 1}$$

Populations structured by size or stage similarly experience costs of variability [5, 6]. There are accordingly two pathways to increase population viability in a variable environment: increase the mean growth rate and/or dampen temporal fluctuation in growth rates, also called “variance buffering”.

Both the characteristics of species and the properties of their environment can buffer demographic fluctuations, including life history traits such as longevity [7, 8], correlations among vital rates [9], transient shifts in population structure [10], the magnitude of environmental variability [11], or the degree of environmental autocorrelation [12, 13]. These factors determine the risks of extinction faced by populations [14] and underlie management strategies promoting ecosystem resilience [15]. Yet little is known about how biotic interactions influence demographic variability or contribute to variance buffering [16].

Most multicellular organisms host symbiotic microbes that affect growth and performance [17, 18], and many of these are vertically transmitted from maternal hosts to offspring [19]. Vertical transmission links the fitness of hosts and symbionts in a feedback loop that selects for mutual benefits [20]. Many vertically-transmitted microbes are mutualistic and protect hosts from stressful environmental conditions including drought, extreme temperatures, or natural enemies [21, 22]. Some of the best studied examples include bacterial symbionts of insects that provide their hosts with thermal tolerance through the production of heat-shock proteins [23], and fungal symbionts of plants that produce anti-herbivore and drought-protective compounds [24–26]. However, these diverse protective symbioses are context-dependent: the magnitude of benefits depends on environmental conditions [27] and thus will vary temporally in a stochastic environment [28]. We hypothesized that context-dependent benefits from symbionts may buffer hosts against variability through strong benefits during harsh periods and neutral or even costly outcomes during benign periods, reducing the impacts of host exposure to extremes and dampening inter-annual variance relative to non-symbiotic hosts. Variance buffering is a previously unexplored mechanism by

1  
2  
3 139 which symbionts may benefit their hosts instead of or in addition to elevating average  
4 fitness, the focus of most previous research.  
5

6 141 We used a combination of long-term field experiments and stochastic demo-  
7 graphic modeling to test the hypothesis that context-dependent benefits of symbiosis  
8 buffer hosts from the fitness costs of environmental stochasticity. We used cool-season  
9 grasses and *Epichloë* fungal endophytes as a tractable experimental model in which  
10 non-symbiotic plants can be derived from naturally symbiotic plants through heat  
11 treatment, providing a contrast of symbiont effects that controls for the confounding  
12 influence of host genetic background. *Epichloë* endophytes are specialized symbionts  
13 growing intercellularly in the aboveground tissue of ~ 30% of *C<sub>3</sub>* grass species [29].  
14 These fungi are primarily transmitted vertically from maternal plants through seeds  
15 [30]. They produce a variety of alkaloids that can protect host plants from natural  
16 enemies [31] and drought stress [32].  
17

18 152 Over 14 years (2007–2021), we collected longitudinal demographic data on the  
19 survival, growth, reproduction, and recruitment of all plants within replicated  
20 endophyte-symbiotic and endophyte-free populations at our field site in southern Indiana,  
21 USA. Through taxonomic replication (seven host-symbiont species pairs) we  
22 aimed to understand whether host life history traits could explain inter-specific vari-  
23 ation in the magnitude of demographic buffering through symbiosis. We used this  
24 long-term data to parameterize stochastic population projection models in a hierar-  
25 chical Bayesian framework. Specifically, we (1) quantified the effect of symbiosis on  
26 the mean and variance of host vital rates (survival, growth and reproduction) and fit-  
27 ness, (2) evaluated the relationship between host life history traits and the magnitude  
28 of symbiont-mediated variance buffering, (3) determined the relative contribution of  
29 symbiont-mediated mean and variance effects to host fitness, and (4) projected how  
30 increased environmental stochasticity (expected under future climates) changes the  
31 importance of variance buffering as a pathway of host-symbiont mutualism.  
32

## 33 167 Materials and Methods 34

### 35 169 Study site and species 36

37 171 This study was conducted at Indiana University's Lilly-Dickey Woods Research and  
38 Teaching Preserve (39.238533, -86.218150) in Brown County, Indiana, USA. This site  
39 is part of the Eastern broadleaf forests of southern Indiana, where the ranges of many  
40 understory cool-season grass species overlap. The experiment focused on seven of these  
41 grasses (*Agrostis perennans*, *Elymus villosus*, *Elymus virginicus*, *Festuca subverticil-*  
42 *lata*, *Lolium arundinaceum*, *Poa alsodes*, and *Poa sylvestris*), each of which hosts a  
43 unique species of *Epichloë* endophyte (Table S1). All are native to eastern North  
44 America except the Eurasian species *L. arundinaceum*.  
45

### 46 180 Endophyte removal, plant propagation, and field set-up 47

48 181 Seeds from naturally symbiotic populations of the seven focal host species were col-  
49 lected during summer-fall 2006 from Lilly-Dickey Woods and the nearby Bayles Road  
50 Teaching and Research Preserve (39.220167, -86.542683). To generate symbiotic (S+)  
51

1  
2  
3 and symbiont-free (S-) plants from the same genetic lineages, seeds from each species  
4 were disinfected with a heat treatment described in Table S1 or left untreated. The heat  
5 treatment created symbiont-free plants by warming seeds to temperatures at which the  
6 fungus becomes inviable but the host seeds can still germinate. Both heat-treated and  
7 untreated seeds were surface sterilized with bleach to remove epiphyllous microbes,  
8 cold stratified for up to 4 weeks, then germinated in a growth chamber before transfer  
9 to the greenhouse at Indiana University where they grew for ~ 8 weeks. We confirmed  
10 endophyte status by staining thin sections of inner leaf sheath with aniline blue and  
11 examining tissue for fungal hyphae at 200X magnification [33]. We established exper-  
12 imental populations with vegetatively propagated clones of similar sizes. By starting  
13 the experiment with plants of similar sizes and the same number of unique genotypes,  
14 we aimed to limit any potential effects of heat treatments on initial plant growth [34].  
15

16 During the fall of 2007 and spring of 2008, we established 10 3x3 m. plots for *A. perennans*,  
17 *E. villosus*, *E. virginicus*, *F. subverticillata*, and *L. arundinaceum* and 18  
18 plots for *P. alsodes* and *P. sylvestris*. Half of the plots were randomly assigned to be  
19 planted with either symbiotic (S+) or symbiont-free (S-) plants, and initiated with  
20 evenly spaced individuals labeled with aluminum tags. In spring 2008, we placed  
21 plastic deer net fencing around each plot to limit deer herbivory and disturbance;  
22 damaged fences were regularly replaced.

### 23 Long-term demographic data collection

24 Each summer (2008–2021) we censused all individuals in each plot for survival,  
25 growth and reproduction, and added new recruits to the census. Plots contained 13.3  
26 individuals/m<sup>2</sup> on average over the course of the experiment. Each census year was a  
27 sample of inter-annual climatic variation (n = 14 years, comprising 13 demographic  
28 transition years). We censused each species during its peak fruiting stage (May: *Poa*  
29 *alsodes*, *Poa sylvestris*; June: *Festuca subverticillata*; July: *Elymus villosus*, *Elymus vir-*  
30 *ginicus*, *Lolium arundinaceum*; September: *Agrostis perennans*), such that the censuses  
31 were pre-breeding and new recruits came from the previous years' seed production.  
32 Leaf litter was cleared out of each plot prior to the census, to aid in locating plants.  
33 For each plant remaining from the previous year, we determined survival, measured  
34 its size as a count of tillers, and collected reproductive data as counts of reproductive  
35 tillers and seed-bearing spikelets on all reproductive tillers to a maximum of three. We  
36 also tagged all unmarked individuals that were recruits from the previous years' seed  
37 production and collected the same demographic data. New recruits typically had one  
38 tiller and were non-reproductive. In 2008 through 2010, we took additional counts of  
39 seeds per inflorescence for all reproducing individuals in the plots to relate inflorescence  
40 and spikelet counts to seed production. In 2018, we stopped collecting data for the  
41 exotic *L. arundinaceum*, which had very high survival and low recruitment, and conse-  
42 quently very low variation across years. In total across 14 years, the dataset included  
43 demographic information for 16,789 individual host-plants and 31,216 transition-year  
44 observations.

45 We expected plots to maintain their endophyte status (symbiotic or symbiont-  
46 free) because these fungal symbionts are almost exclusively vertically transmitted,  
47 and plots were spaced a minimum of 5 m apart, limiting seed dispersal or horizontal  
48

1  
2  
3 transmission of the symbiont between plots. However, we regularly confirmed endo-  
4 phyte treatment throughout the lifetime of the experiment by opportunistically taking  
5 subsets of seeds from reproductive individuals and scoring them for their endophyte  
6 status with microscopy as above. Overall, these scores reflected 98% faithfulness of  
7 recruits to their expected endophyte status across species and plots (Fig. S23; Sup-  
8 plement data). Additionally, we have rarely observed fungal stromata, the fruiting  
9 bodies by which *Epichloë* are potentially transmitted horizontally, provided the fly  
10 vector is also present [35]. For *A. perennans*, *F. subverticillata*, *L. arundinaceum*, and  
11 *P. alsodes*, we never observed stromata. We observed stromata only infrequently for  
12 *E. villosus*, and even more rarely for *E. virginicus* and *P. sylvestris* (Table S2). For  
13 these species, stromata have only been observed irregularly across years on 35, 4, and  
14 6 plants respectively, making up < 0.3% of all censused plants.  
15  
16

#### 243 244 Vital rate modeling

18 Equipped with these demographic data, we fit statistical models for survival, growth,  
19 flowering (yes or no), fertility of flowering plants (number of flowering tillers), pro-  
20 duction of seed-bearing spikelets (number per inflorescence), the average number of  
21 seeds per spikelet, and the recruitment of seedlings from the preceding year's seed  
22 production. We fit these vital rates as generalized linear mixed models in a hierar-  
23 chical Bayesian framework using RStan [36] which allowed us to isolate endophyte  
24 effects on vital rate means and variances, borrow strength across species for some  
25 variance components, and propagate uncertainty from the individual-level vital rates  
26 to population projection models [37]. All vital rate models included random plot  
27 and year effects, with separate estimates of year-to-year variance for symbiotic and  
28 symbiont-free plants, to quantify the effect of endophytes on inter-annual variance.  
29 All parameters were given vague priors [38]. We ran each vital rate model for 2500  
30 warm-up and 2500 MCMC sampling iterations with three chains. We assessed model  
31 convergence with trace plots of posterior chains and checked for  $\hat{R}$  values less than  
32 1.01, indicating low within- and between-chain variation [39, 40]. For those models  
33 that showed poor convergence, we extended the MCMC sampling to include 5000  
34 warm-up and 5000 sampling iterations, which was only necessary for seedling growth.  
35 We graphically checked vital rate model fit with posterior predictive checks comparing  
36 simulated and observed data (Fig. S19-S20).  
37

38 *Survival* - We modeled survival as a Bernoulli process, where the survival ( $S$ ) of  
39 an individual  $i$  in plot  $p$  and census year  $t$  was predicted by the plot-level endophyte  
40 status ( $e$ ), host species ( $h$ ), size in the preceding census, and the plant's origin status  
41 (whether it was initially transplanted or naturally recruited into the plot).

$$S_{i,p,e,h,t} \sim Bernoulli(\hat{S}_{i,p,e,h,t}) \quad (2a)$$

$$\text{logit}(\hat{S}_{i,p,e,h,t}) = \beta_{0_h} + \beta_1 * \text{origin}_i \quad (2b)$$

$$+ \beta_{2_h} * \text{endo}_e + \beta_{3_h} * \text{size}_{i,t-1} + \tau_{e,h,t} + \rho_p \quad (2c)$$

$$\tau_{e,h,t} \sim Normal(0, \sigma_{\tau_{e,h}}^2) \quad (2d)$$

1  
2  
3                    $\rho_p \sim Normal(0, \sigma_{\rho}^2)$                    (2e)                   277  
4  
5  
6  
7  
8  
9  
10  
11  
12  
13  
14  
15

278  
279  
280  
281  
282  
283  
284  
285  
286  
287  
288  
289  
290  
291  
292  
293  
294  
295  
296  
297  
298  
299  
300  
301  
302  
303  
304  
305  
306  
307  
308  
309  
310  
311  
312  
313  
314  
315  
316  
317  
318  
319  
320  
321  
322

Here,  $\hat{S}$  is the survival probability,  $\beta_{0_h}$  is an intercept specific to each host species,  $\beta_1$  is the effect of the plant's recruitment origin,  $\beta_{2_h}$  is the endophyte effect,  $\beta_{3_h}$  is the size effect,  $\tau_{e,h,t}$  is a normally distributed year effect for each species and endophyte status with variance  $\sigma_{\tau_{e,h}}^2$ , and  $\rho_p$  is a normally distributed plot effect with variance  $\sigma_{\rho}^2$  ( $p(e)$  indicates that plot identity is uniquely associated with an endophyte status). We assume that origin effect  $\beta_1$  and plot-to-plot variance  $\sigma_{\rho}^2$  are shared across host species, allowing us to "borrow strength" across the multi-species dataset; other model parameters are unique to host species. We separately modeled the survival of newly recruited seedlings with a similar model but omitting previous size dependence and origin status.

*Growth* - We modeled plant size in census year  $t$  ( $G$ ) with the same linear predictor for the mean as described for survival. Because we measured size as positive integer-valued counts of tillers, we modeled it with a zero-truncated Poisson-inverse Gaussian distribution. This distribution includes a shape parameter  $\lambda_G$  to account for overdispersion in the data. We additionally modeled the growth of newly recruited seedlings separately with a Poisson-inverse Gaussian model omitting size structure and the plants' origin status as with seedling survival.

*Flowering* - We modeled whether or not a plant was flowering during the census ( $P$ ) as a Bernoulli process, with the same linear predictor for the mean as described above for survival except that size dependence for reproductive vital rates was determined by the individual's size during the same census year as opposed to its size during the previous year.

*Fertility* - For a plant that was flowering during the census, its fertility was the number of reproductive tillers produced ( $F$ ), which we modeled as a function of size in the same census period with a zero-truncated Poisson-Inverse Gaussian distribution, with the same linear predictor for the mean as described above.

*Spikelets per Inflorescence* - Spikelet production ( $K$ ) was recorded as integer counts on up to three inflorescences per reproducing plant. We modeled these data with a negative binomial distribution, with the same linear predictor for the mean as described above.

*Seed Production per Spikelet* - For individuals with recorded counts of seed production, we calculated the number of seeds per spikelet from our counts of seeds and spikelets per inflorescence, and then modeled seeds per spikelet ( $D$ ) as means of a Gaussian distribution for each species and endophyte status. Because we had less detailed data across years and plants for seed production than for other reproductive vital rates, we omitted both plot and year random effects.

*Seedling Recruitment* - We used a binomial distribution to model the recruitment of new seedlings ( $R$ ) into the plots from seeds produced in the preceding year, assuming no long-lived seed bank. We included an intercept specific to each host and endophyte status and the same random effects structure as in other models. We estimated the number of seeds per plot in the preceding year by multiplying the total number of reproductive tillers per plant by the mean number of spikelets per inflorescence and mean number of seeds per spikelet ( $D$ ). For plants with missing fertility or spikelet

1  
2  
3 data, we used the expected number of reproductive tillers ( $F$ ) or of spikelets per  
4 inflorescence from ( $K$ ), drawing from the full posteriors of our models. We rounded  
5 this value to get the estimated seed production for each individual, and finally summed  
6 across all reproductive plants in each year and plot to get the total number of seeds  
7 produced.  
8

9     328 **Stochastic population model**  
10    329

11    330 Using the fitted vital rate models, we parameterized stochastic matrix projection mod-  
12    331 els including two state variables:  $r_t$  (the number of newly recruited individuals in year  
13    332  $t$ ), and  $\mathbf{n}_t$  (a vector including all non-seedling individuals of sizes  $x \in \{1, 2, \dots, U\}$ , rang-  
14    333 ing from one to the maximum number of tillers  $U$ ). We use these two state variables to  
15    334 avoid having to assume demographic equivalence between seedling and non-seedling  
16    335 one-tiller plants. We used the same model structure for each species and endophyte  
17    336 status (not shown in model notation, to make it more readable).  
18

19    338     The number of recruits in year  $t + 1$  is given by:  
20

21    339     340 
$$r_{t+1} = \sum_{x=1}^U P(x; \boldsymbol{\tau}_P) F(x; \boldsymbol{\tau}_F) K(x; \boldsymbol{\tau}_K) DR(\boldsymbol{\tau}_R) n_t^x \quad (3)$$
  
22    341

23    342 The total number of seeds produced by a maternal plant of size  $x$  is the product  
24    343 of the size-specific probability of flowering  $P$ , the number of reproductive tillers  $F$ ,  
25    344 the number of spikelets per inflorescence  $K$ , and the number of seeds per spikelet  $D$ .  
26    345 Multiplying by the probability of transitioning from seed to seedling  $R$  gives a per-  
27    346 capita rate of seedling production, which is multiplied by the number of plants of size  
28    347  $x$  ( $n_t^x$ , the  $x^{\text{th}}$  element of  $\mathbf{n}_t$ ) and summed over all sizes. Each function also depends  
29    348 on the species- and endophyte-specific year random effects for that vital rate ( $\boldsymbol{\tau}$ , a  
30    349 vector of year-specific values derived from the statistical models).  
31

32    350     The number of  $y$ -sized plants in year  $t + 1$  is given by:  
33

34    351     352 
$$n_{t+1}^y = Z(y; \boldsymbol{\tau}_Z) B(\boldsymbol{\tau}_B) r_t + \sum_{x=1}^U S(x; \boldsymbol{\tau}_S) G(x, y; \boldsymbol{\tau}_G) n_t^x \quad (4)$$
  
35    353

36    354 where  $n_{t+1}^y$  is the  $y^{\text{th}}$  element of vector  $\mathbf{n}_{t+1}$ . The first term on the right hand side of  
37    355 Eqn. 4 represents growth ( $Z$ ) and survival ( $B$ ) of seedling recruits. The second term  
38    356 includes the survival of previously  $x$ -sized plants and the growth of survivors from size  
39    357  $x$  to  $y$ , summed over all  $x$ . To avoid predictions of unrealistic growth outside of the  
40    358 observed size distribution, we set a ceiling on the growth function for plants at the  
41    359 97.5<sup>th</sup> percentile of observed sizes for each host species [41].  
42

43    360     Each of the vital rate functions in Eqns. 3 and 4 have separate intercepts and year  
44    361 random effects for symbiotic and symbiont-free populations, allowing us to calculate  
45    362 the effect of endophyte symbiosis on the mean, variance, and coefficient of variation  
46    363 (CV) of  $\lambda$ , the dominant eigenvalue of the year- and endophyte-specific projection  
47    364 matrix. This model treats climate drivers implicitly through year-specific random  
48    365 effects. We also developed a climate-explicit version with the addition of parameters  
49    366 defining the relationship between either annual or growing season drought index and  
50

each vital rate. A full description of climate-explicit methods can be found in the *Supporting Information Supplemental Methods*. 369  
370  
371

## Life History Analysis

We collected metrics describing each host species' life history to test the relationship between pace of life and variance buffering (Table S1). Using the Rage package [42], we calculated  $R_0$ , longevity, and generation time from our estimated transition matrices using the symbiont-free mean matrix as the reference condition. We recorded seed size as the average lemma length from the Flora of North America [43]. We also calculated the 99th percentile of maximum observed age for each species from their S- populations. Next, we fit Bayesian phylogenetic mixed-effects models using the brms package [44] to test the relationship between each life history trait and the effect of symbiosis on the CV of  $\lambda$  (a measure of variance buffering) while controlling for phylogenetic non-independence between host and symbiont species. We pruned species-level phylogenies of plants [45] and *Epichloë* fungi [46] to include the focal species. *Agrostis perennans* was not included in the tree, and so we used the congener *A. hyemalis*. We defined separate phylogenetic covariance matrices for each pruned tree. We propagated uncertainty in the estimated variance buffering effect  $V$  with a measurement error model:

$$\begin{aligned}
 V_{MEAN,h} &\sim Normal(V_{EST,h}, V_{SD,h}) & (5a) \\
 V_{EST,h} &\sim Normal(\mu_h, \sigma) & (5b) \\
 \mu &= \alpha + \beta * trait + \pi_j & (5c) \\
 \alpha &\sim Normal(0, .5) & (5d) \\
 \beta &\sim Normal(0, .1) & (5e) \\
 \sigma &\sim Half - Normal(.04, .01) & (5f) \\
 \pi_h &\sim MVN(0, \sigma_\pi \mathbf{A}) & (5g) \\
 \sigma_\pi &\sim Half - Normal(0, .1) & (5h)
 \end{aligned}$$

Here,  $V_{EST}$  is the variance buffering effect for host species  $h$ , estimated from the posterior mean ( $V_{MEAN}$ ) and standard deviation ( $V_{SD}$ ), propagating uncertainty associated with the effect of symbiosis. The model includes an intercept ( $\alpha$ ) and a slope ( $\beta$ ) defining the relationship between the variance buffering effect and the life history trait. The residual standard deviation is given by ( $\sigma$ ). We used weakly informative priors to aid model convergence. Each prior was centered at zero, except for the residual standard deviation, which we centered at the standard deviation of the estimated variance buffering effect, .04. The phylogenetic random effect ( $\pi$ ), which is modeled as a multivariate normal distribution, has a between-species standard deviation ( $\sigma_\pi$ ) structured by the phylogenetic covariance matrix  $\mathbf{A}$ . We ran each MCMC sampling chain for 8000 warmup iterations and 2000 sampling iterations. We assessed model convergence as described for the vital rate models.

### 415 Mean-variance decomposition

416 To calculate stochastic population growth rates ( $\lambda_s$ ) for each host species and endo-  
417 phyte status we simulated population dynamics for 1000 years by randomly sampling  
418 from the 13 annual transition matrices, discarding the first 100 years to minimize  
419 the influence of initial conditions. Sampling observed transition matrices produces  
420 models that realistically capture inter-annual variation by preserving correlations  
421 between vital rates [47]. We tallied the total population size at each time step as  
422  $N_t = r_t + \sum_{x=1}^U n_t^x$  and calculated the stochastic growth rate as  $\log(\lambda_s) = E[\log(\frac{N_t}{N_{t+1}})]$   
423 [48, 49]. We calculated the total effect of endophyte symbiosis as the difference in  $\lambda_s$   
424 between S+ and S- populations. We propagated uncertainty from the vital rate mod-  
425 els to the calculation of  $\lambda_s$  using 500 draws from the posterior distribution of model  
426 parameters.

427 We decomposed the total endophyte effect on  $\lambda_s$  into contributions from effects  
428 on vital rate means, variances, and their interaction. Specifically, we repeated the  
429 calculation of  $\lambda_s$  for two additional “treatments”: (1) endophyte effects on mean vital  
430 rates only, with inter-annual variances shared between S+ and S- at the S- reference  
431 level for all vital rates, and (2) endophyte effects on vital rate variances only, with  
432 vital rate means shared between S+ and S- at the S- reference level. The combination  
433 of all four  $\lambda_s$  treatments (S+ vital rate means and variances, S- means and variances,  
434 S+ means with S- variances, S- means with S+ variances) allowed us to quantify to  
435 what extent the overall effect of symbiosis derives from changes in vital rates means,  
436 variances, and their interaction. The interaction occurs because the variance penalty  
437 to stochastic growth is proportional to the mean value of annual growth rates (see Eq.  
438 1) such that variance is more detrimental for populations with lower average growth  
439 rates.

440 To create scenarios of increased variance relative to that observed during the study  
441 period, we repeated the stochastic growth rate decomposition, but sampling only a  
442 subset of the 13 observed annual transition matrices. We created two scenarios of  
443 increased environmental variance by sampling the transition matrices associated with  
444 the six or two most extreme  $\lambda$  values, representing the six or two best and worst years,  
445 using S- populations as the reference condition. By sampling away from an average  
446 year in both directions, the six- and two- years scenarios increased the standard devi-  
447 ation of yearly host growth rates by 1.3 and 2.1 times, respectively, without changing  
448 mean growth rates (< 2.3% difference in  $\bar{\lambda}$  between simulation treatments, Fig. S21).  
449 We performed the same mean-variance decomposition for these scenarios as for the  
450 ambient conditions (all 13 years sampled) for all host species described above.

## 453 Results and Discussion

### 455 Symbionts buffer host demographic variance

456 Across seven host species, eight vital rates, 14 years, and 16,789 individual plants, our  
457 analysis provided the first empirical evidence of symbiont-mediated variance buffer-  
458 ing. Endophytes reduced inter-annual variance for 66% (37/56) of host species-vital  
459 rate combinations (average Cohen’s D for effects on vital rate standard deviation:  
460

1  
2  
3 –0.15) (Fig 1A; Fig. S6 - Fig. S18). Endophytes also increased mean vital rates for  
4 the majority (36/56) of host species-vital rate combinations (average Cohen's D for  
5 effects on vital rate mean: 0.15), and benefits were particularly strong for host sur-  
6 vival, plant growth and recruitment (Fig. 1A; Fig. S1 - Fig. S5). The magnitude of  
7 mean and variance effects differed among host species and vital rates. For example,  
8 endophytes modestly increased mean adult survival (Fig. 1C) and reduced variance in  
9 survival (Fig. 1D) for *Festuca subverticillata*, while for *Poa alsodes*, variance buffer-  
10 ing was more apparent in seedling growth and inflorescence production (Fig 1E).  
11 Interestingly, certain vital rates showed costs of endophyte symbiosis. Symbiotic indi-  
12 viduals of *A. perennans* grew larger than those without endophytes (Fig. 1B), yet  
13 endophytes also reduced this species' mean recruitment rates (Fig. 1A). In addition,  
14 endophyte symbiosis increased variance in seedling growth for *Elymus villosus* and  
15 *Festuca subverticillata* (Fig. 1A).

16 Because not all vital rates contribute equally to fitness, we used stochastic matrix  
17 models to integrate the diverse effects on vital rates described above into comprehen-  
18 sive measures for the mean and variance of year-to-year fitness ( $\lambda_t$ ) and the long-run  
19 stochastic fitness that integrates both mean and variance ( $\lambda_S$ ). On average across host  
20 species, S+ populations had greater mean fitness (> 92% confidence that endophytes  
21 increased  $\bar{\lambda}$ ) and lower inter-annual variability in fitness (> 86% confidence that endo-  
22 phytes decreased the coefficient of variation of  $\lambda_t$ ) than S- populations (Fig. 2). For  
23 some host species, the CV of  $\lambda_t$  declined by as much as 170% (*P. alsodes*, *F. subverti-*  
24 *cillata*), while for others, endophyte effects on variance were substantially smaller (6%  
25 lower for *E. villosus*, 16% lower for *A. perennans*), or even positive (27% increase for  
26 *E. virginicus*). When mean and variance effects of symbionts were considered together,  
27 none of the host-symbiont pairings were antagonistic (i.e., with endophytes that both  
28 decreased mean fitness and increased variance) (Fig. 2C), suggesting that variation  
29 across host species and vital rates in mean and variance effects may reflect alternative  
30 strategies that yield similar net benefits of endophyte symbiosis.

31 Reduced sensitivity to drought, as has been reported for some *Epichloë* symbioses  
32 [32], is a candidate mechanism that could generate a signature of variance buffering:  
33 drought conditions may have weaker fitness costs for S+ hosts, reducing fluctuations in  
34 fitness through time. Accordingly, analysis of climate-explicit matrix models indicated  
35 that, for five of seven taxa, S+ populations were less sensitive to annual or growing  
36 season drought (12-month or 3- month drought index; Standardized Precipitation-  
37 Evapotranspiration Index [50]) than S- populations (Supporting Information Text;  
38 Fig. S24-S25; Table S3). However, we did not find a strong relationship between the  
39 magnitude of variance buffering and relative drought sensitivities, suggesting that  
40 other climatic factors or other temporally-varying aspects of the environment may  
41 elicit benefits of endophyte symbiosis, including documented resistance to herbivory  
42 for six of these host taxa [51, 52].

#### 44 Faster life histories predict stronger symbiont-mediated 45 variance buffering

46 Theory predicts that long-lived species, those on the slow end of the slow-fast life  
47 history continuum, will be less sensitive to environmental variability than short-lived  
48

1  
2  
3 species [53], a pattern which has empirical support across plants [54] and animals  
4 [8, 55]. Therefore, host species with long lifespans that produce few, large offspring  
5 should benefit less from symbiont-mediated variance buffering than species with fast  
6 life cycles that produce many smaller offspring with low per-capita chance of success  
7 [56, 57]. In support of this prediction, hosts with trait values representing faster life  
8 history strategies experienced greater variance buffering from endophytes than those  
9 with slow life histories (Fig. 3). Bayesian phylogenetic mixed-effects models, controlling  
10 for species' relatedness, indicated that variance buffering was stronger for host species  
11 with shorter lifespan (Fig. 3A; 75% probability of positive relationship with empirically  
12 observed maximum plant age) and smaller seeds (Fig. 3B; 73% probability of positive  
13 relationship with seed length). Other life history traits similarly had positive, but  
14 weaker, support for the prediction that faster life history traits correlate with stronger  
15 variance buffering (Fig. S26-S28). Considering fungal life history traits, the three host  
16 species for which the net mutualism benefit was weakest (*Elymus villosus*, *Elymus*  
17 *virginicus*, and *Poa sylvestris*) (Fig. 2C) were the only hosts for which we observed  
18 fungal stromata, fruiting bodies capable of horizontal (contagious) transmission (Table  
19 S2). This result supports the theoretical expectation that strict vertical transmission  
20 drives the evolution of strong host-symbiont mutualism [20, 58]. Conclusions about  
21 life histories are somewhat constrained by the narrow range of trait values among  
22 closely related species in the grass sub-family Pooideae and their co-evolving symbionts.  
23 Our understanding of how life history variation modulates the fitness consequences of  
24 microbial symbiosis would profit from tests across a wider span of taxonomic groups  
25 [59].  
26  
27

### 28 531 Contributions from variance buffering are weak relative to 29 532 mean effects



30 To evaluate the relative importance of mean fitness benefits and variance buffering as  
31 alternative pathways of mutualism, we decomposed the overall effect of the symbiosis  
32 on the stochastic growth rate  $\lambda_S$  using simulations from the population models in four  
33 configurations. These included either the full symbiosis effect (both mean and variance  
34 buffering effects), mean effects alone, variance effects alone, or neither mean nor vari-  
35 ance effects. Overall, the full effect of symbiosis on  $\lambda_S$ , averaged across host species,  
36 provided strong evidence of grass-endophyte mutualism (99% certainty of a positive  
37 total effect on  $\lambda_s$ ) (Fig. 4; see Fig. S22 for individual host species). Contributions to  
38 this full effect derived from both mean and variance buffering effects, as well as a  
39 slightly negative interaction (i.e., the combined influence of mean and variance effects  
40 was smaller than the sum of their individual effects). Endophytes' contributions to  $\lambda_S$   
41 from mean effects were four times greater, averaged across species, than contributions  
42 from variance buffering (Fig. 4), suggesting that, under the regime of environmen-  
43 tal variability represented by our 14-year study, dampened fluctuations in fitness via  
44 variance buffering was a far less important element of the benefits of symbiosis than  
45 increased mean fitness. Results for individual host species were largely consistent with  
46 the cross-species trends (Fig S22). The full effect of symbiosis on  $\lambda_S$  was positive for  
47 seven out of eight host species, with statistical confidence ranging from 66% to > 99%  
48 certainty. The one exception was the host species *P. sylvestris*, for which our analysis  
49

1  
2  
3 indicated that fungal endophytes were effectively neutral in their overall fitness effect 553  
4 (45% and 55% posterior probability of positive and negative effects; Fig S22). 554  
5  
555

## 6 Variance buffering strengthens under increased environmental 556 7 variability 557 8

9 Simulations of increased environmental variability, a key prediction of climate change 558  
10 forecasts [2], indicated that mutualism with microbial symbionts, and their variance 559  
11 buffering effects in particular, will take on increased importance for hosts in a more 560  
12 variable future climate. To simulate increased variability, we repeated the decomposition 561  
13 of  $\lambda_S$  for two alternative forecast scenarios, randomly sampling transition matrices 562  
14 that represented either the six most extreme years experienced by each species or the 563  
15 two most extreme years, subsets of the thirteen transition matrices across the 14-year 564  
16 study period. Increased variability elicited stronger mutualistic benefits of endophyte 565  
17 symbiosis (Fig. 3) than ambient variability (overall effect of the symbiosis increased 566  
18 by > 130%). This increase was driven by increased contributions from the variance 567  
19 buffering mechanism (from a 24% contribution in the ambient scenario to a 66% con- 568  
20 tribution in the most variable scenario) rather than from greater mean effects. In the 569  
21 most variable scenario, the relative importance of mean and variance effects reversed, 570  
22 with variance buffering contributions that were 1.5 times greater than contributions 571  
23 from mean benefits, averaged across species (Fig. 4). Thus, variance buffering – a cryp- 572  
24 tic microbial influence that manifests only over long time scales – is poised to become 573  
25 the dominant way in which grasses benefit from symbiosis with fungal endophytes in 574  
26 more variable climates of the future. 575  
27  
28

## Conclusion 576 29

30 Ecologists increasingly recognize the importance of symbiotic microbes for host organisms 577  
31 and the populations, communities, and ecosystems in which their hosts reside 578  
32 [60–63]. Despite awareness of these ubiquitous interactions, long-term studies of micro- 579  
33 bial symbiosis are very rare. Our analysis of taxonomically-replicated, long-term field 580  
34 experiments that manipulated the presence/absence of fungal symbionts in plants 581  
35 demonstrates for the first time that heritable microbes can commonly benefit hosts 582  
36 not only through improved mean fitness – the focus of most previous research – but 583  
37 also through buffering against environmental variance. Our results provide an impor- 584  
38 tant advance to improve forecasts of the responses of populations (and symbionts) 585  
39 to increasing environmental stochasticity under global change, suggesting that, for 586  
40 some host species, microbial symbiosis may compensate for the lack of intrinsic toler- 587  
41 ance of variability conferred by “slow” life history traits. We found that, relative to 588  
42 mean fitness benefits, symbiont-mediated variance buffering made weak contributions 589  
43 to host-symbiont mutualism under the current regime of environmental variability. 590  
44 However, variance buffering is likely to become the dominant benefit that fungal 591  
45 endophytes confer to grass hosts in more variable future environments. This result 592  
46 emerges from the context-dependent nature of grass-endophyte interactions, combined 593  
47 594  
48 595  
49 596  
50 597  
51 598

1  
2  
3 599 with the observation that environmental stochasticity generates fluctuation in con-  
4 text. These key ingredients, and thus the potential for symbiont-mediated variance  
5 buffering, similarly apply to the diverse host-microbe symbioses across the tree of life.  
6  
7  
8  
9  
10  
11  
12  
13  
14  
15  
16  
17  
18  
19  
20  
21  
22  
23  
24  
25  
26  
27  
28  
29  
30  
31  
32  
33  
34  
35  
36  
37  
38  
39  
40  
41  
42  
43  
44  
45  
46  
47  
48  
49  
50  
51  
52  
53  
54  
55  
56  
57  
58  
59  
60



1  
2  
3      **Acknowledgments.** We thank Mark Sheehan, Ali Campbell, Kyle Dickens, Blaise      645  
4      Willis, and Sar Lindner for contributions to field data collection. We also thank Volker      646  
5      Rudolf, Daniel Kowal, Lydia Beaudrot and Judie Bronstein for helpful comments on      647  
6      and discussion of this project. This research was supported by the National Science      648  
7      Foundation (grants 1754468 and 2208857).      649  
8

9      **Supplementary information.** Supplementary information for this paper includes  
10     Supplementary Methods, Figs. A1 to A28, and Tables A1 to A3.      650  
11                          651  
12                          652  
13                          653  
14                          654  
15                          655  
16                          656  
17                          657  
18                          658  
19                          659  
20                          660  
21                          661  
22                          662  
23                          663  
24                          664  
25                          665  
26                          666  
27                          667  
28                          668  
29                          669  
30                          670  
31                          671  
32                          672  
33                          673  
34                          674  
35                          675  
36                          676  
37                          677  
38                          678  
39                          679  
40                          680  
41                          681  
42                          682  
43                          683  
44                          684  
45                          685  
46                          686  
47                          687  
48                          688  
49                          689  
50                          690  
51                          691

1  
2  
3  
4  
5  
6  
7  
8  
9  
10  
11  
12  
13  
14  
15  
16  
17  
18  
19  
20  
21  
22  
23  
24  
25  
26  
27  
28  
29  
30  
31  
32  
33  
34  
35  
36  
37  
38  
39  
40  
41  
42  
43  
44  
45  
46  
47  
48  
49  
50  
51  
52  
53  
54  
55  
56  
57  
58  
59  
60

## Figures

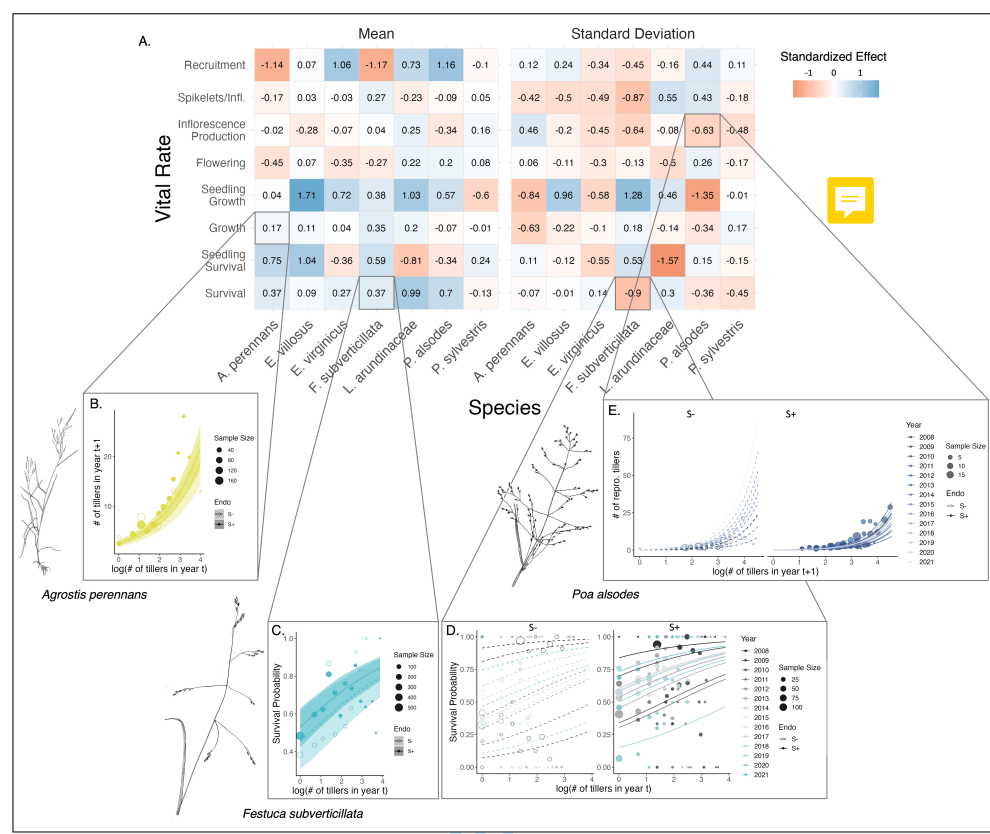


**Fig. 1** Endophyte symbiosis altered host vital rates.(A) Shading represents the posterior mean standardized effect size (Cohen's D) of endophyte symbiosis on mean or standard deviation of host vital rates (blue indicates that symbiosis increased the mean or standard deviation and red indicates a reduction). Endophytes' diverse vital rate effects include increased (B) mean growth of *A. perennans* and (C) mean survival probability of *F. subverticillata*. Endophyte presence also reduced inter-annual variance in (D) the survival of *F. subverticillata* and (E) the fertility of *P. alsodes*. In panels B-C, mean vital rate estimates are shown with 80% credibles along with data binned by size for symbiotic (S+) and symbiont-free (S-) plants, while in panels D-E, annual vital rate estimates are shown along with data binned by size and census year. Organism silhouettes modified from "Festuca subverticillata" by Cindy Roché and "Agrostis hyemalis" and "Poa alsodes" by Sandy Long ©Utah State University.

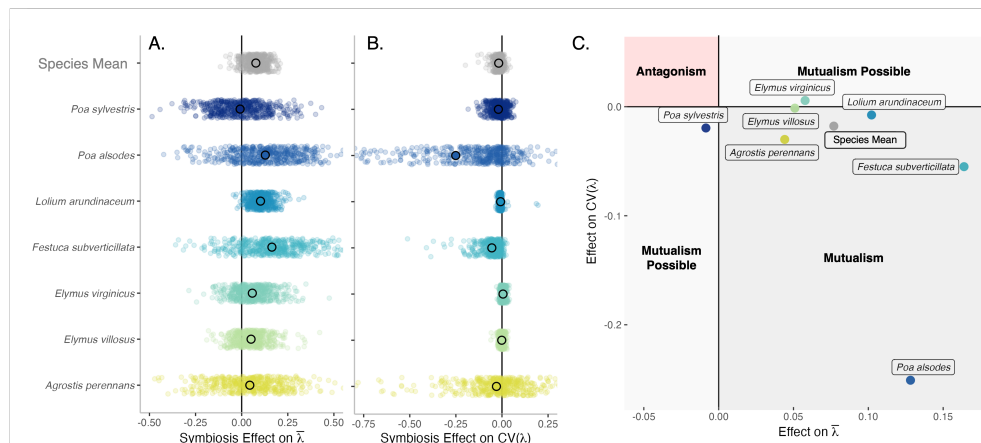


**Fig. 2** Mean and variance-buffering effects on fitness. Black circles indicate the average effect of endophytes along with 500 posterior draws (smaller colored circles) on the (A) mean and (B) coefficient of variation in  $\lambda$  for each host species as well as a cross species mean. (C) For all hosts, endophytes either reduce variance, increase the mean, or both, and consequently when considering stochastic environments, the interactions are always at least potentially mutualistic.

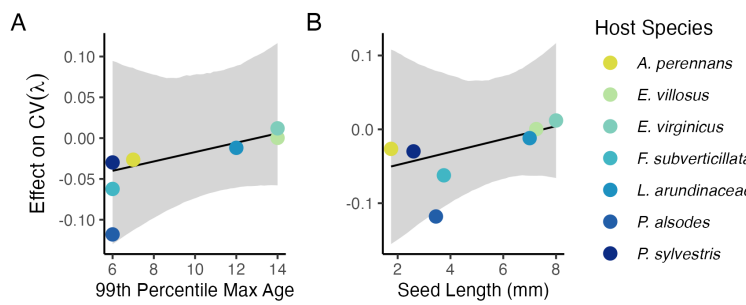


**Fig. 3** Host species with faster life history traits experience stronger effects of symbiont-mediated variance buffering. Regressions between life history traits describing the fast-slow life history continuum ((A) 99th percentile maximum age observed during long term censuses in years; (B) Seed size) and the effect of endophyte symbiosis on the coefficient of variation in population growth rate ( $\lambda$ ). Each panel shows the fitted mean relationship (line) along with the 95% credible interval.

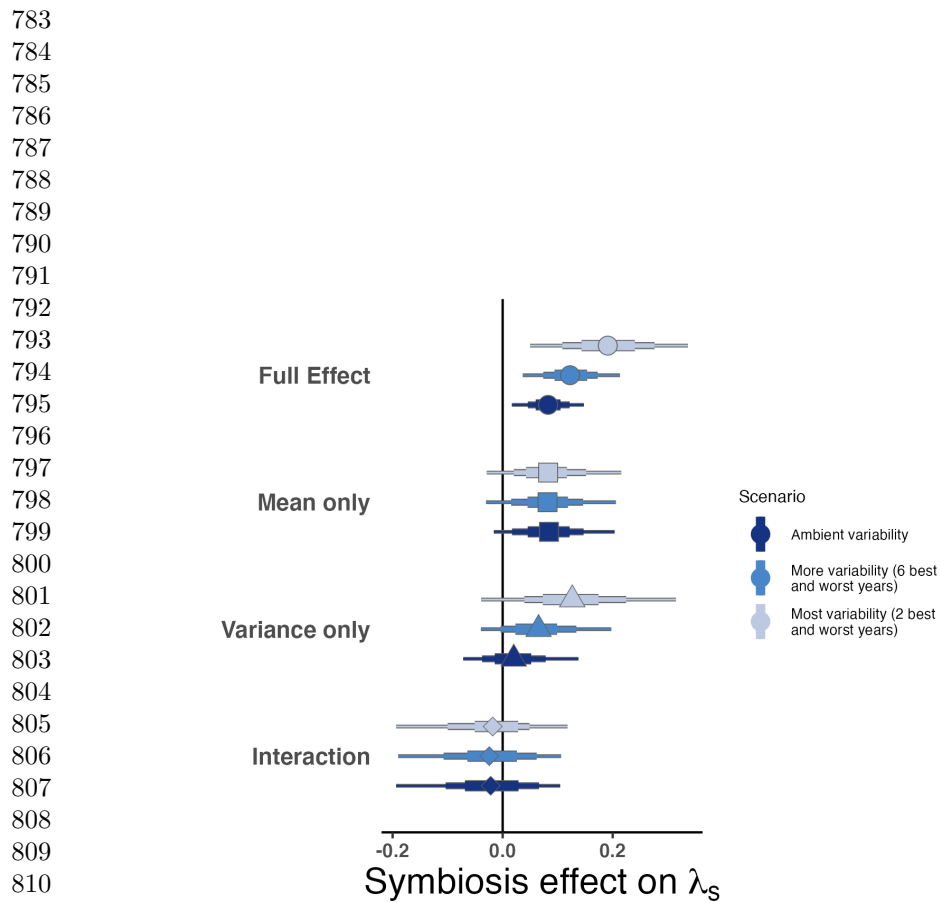


**Fig. 4** Cross-species average endophyte contributions to stochastic growth rates under observed and elevated variance. Endophyte symbiosis contributes to the total effect of mutualism on  $\lambda_s$  through benefits to mean growth rates and through variance buffering as well as the interaction between mean and variance effects. Shapes indicate the posterior mean of each contribution averaged across the seven focal symbiota, along with bars for the 50, 75 and 95% credible intervals. The full effect of the symbiosis (circles) becomes more mutualistic under scenarios of increased variance (represented by color shading). Relative to the ambient scenario sampling transition matrices for all 13 transition years during the study period, simulations increased variance by sampling the most extreme six or two years years, leading to increased contributions from variance buffering effects (triangles) and a constant contribution from mean effects (squares).

1  
2  
3     **Supporting Information**    829  
4  
56     **Supplemental Methods**    830  
7  
89       **Estimating climate drivers of environmental context-dependence**    831  
10  
11  
12  
13  
14  
15  
16  
17  
18  
19  
20  
21  
22  
23  
24  
25  
26  
27  
28  
29  
30  
31  
32  
33  
34  
35  
36  
37  
38  
39  
40  
41  
42  
43  
44  
45  
46  
47  
48  
49  
50  
51  
52  
53  
54  
55  
56  
57  
58  
59  
60

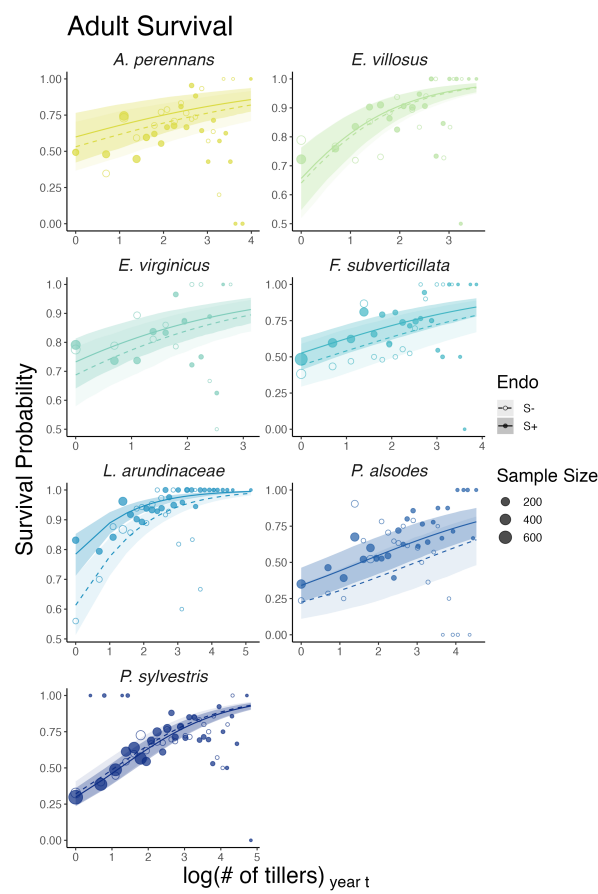
To connect the variance buffering effects of endophytes with inter-annual variability in climate, we built climate-explicit stochastic matrix population models from the vital rate data in addition to the climate-implicit model described in the main text. Identifying the potentially complex relationships between vital rates and environmental drivers remains a key challenge for accurate forecasts of the ecological impacts of environmental stochasticity [64]. We first downloaded temperature and precipitation data from a weather station in Bloomington, IN, approx. 27 km from our study site, using the rnoaa package [65]. Compared to other weather stations in the area, the measurements from Bloomington contain the most complete climate record across the study period and are correlated with more local measurements from Nashville, IN for years in which local data are available (total daily precipitation:  $R^2 = .76$ ; mean daily temperature:  $R^2 = .94$ ). The mean annual temperature across the study period was  $11.9 C^\circ$  (SD:  $1.05 C^\circ$ ) and the average annual precipitation was 1237.9 mm/year (SD: 204.89 mm/year) (Fig. S24). Given the known role of endophytes in promoting host drought tolerance, we calculated the Standardised Precipitation-Evapotranspiration Index (SPEI) for 3 and 12 months preceding each annual censuses, reflecting drought during the growing season and across the year [50]. To calculate SPEI, we used the Thornthwaite equation to model potential evapotranspiration as implemented in the SPEI R package [66]

We repeated the process of fitting statistical models for each vital rate as described in **Materials and Methods** with the inclusion of a parameter describing the influence of SPEI. We fit separate vital rate models incorporating either the growing season or annual drought index for each vital rate, except for the model describing the mean number of seeds per inflorescence. This model was fit without climate effects because the data came from only a few years. Initial analyses indicated similar fits for models including only a linear term and those with both linear and quadratic terms describing the relationship between the climate driver and the vital rate response, and so we proceeded with models including only the linear term. We expected that including climate predictors into the models would explain some inter-annual variance in vital rates, shrinking the variance associated with the fitted year random effects. We assessed model fit with graphic posterior predictive checks and convergence diagnostics as described for the climate-implicit analysis. Finally, we next built matrix projection models incorporating the climate-dependent vital rate functions to assess the response of symbiotic (S+) vs symbiont-free (S-) populations to drought. The model is as described in **Materials and Methods** with the inclusion of parameters describing the slope of the relationship with SPEI. We compared the sensitivity of  $\lambda$  to either annual or seasonal SPEI of S+ populations ( $\frac{\Delta\lambda^+}{\Delta SPEI}$ ) with those of S- populations ( $\frac{\Delta\lambda^-}{\Delta SPEI}$ ) (Fig. S25; Table S).

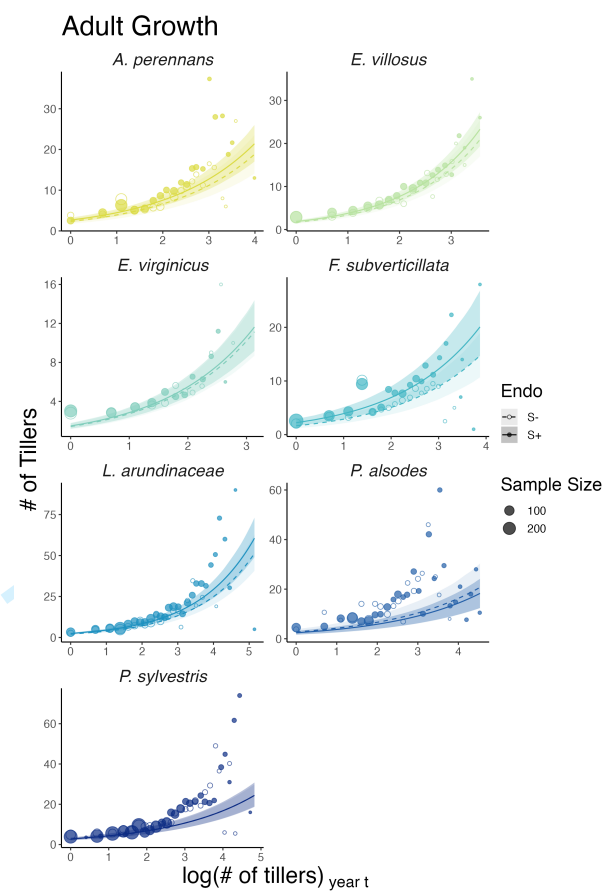
Most species were slightly more responsive to growing season rather than annual drought conditions, and for most species symbiotic populations were less sensitive to

1  
2  
3 SPEI than symbiont-free populations (Fig. S25; Table S3). However, these drought  
4 indices did not explain the full extent of inter-annual variability in demographic  
5 vital rates. For example, flowering in *A. perennans* had one of the strongest climate  
6 signals (82% probability of a positive relationship with SPEI), yet the estimated inter-  
7 annual variance  $\sigma_{\tau_p}^2$  for symbiont-free plants shrank from 6.7 to 6.1 after including  
8 3-month SPEI as a covariate, suggesting that other factors contribute to inter-annual  
9 variability.  
10  
11  
12  
13  
14  
15  
16  
17  
18  
19  
20  
21  
22  
23  
24  
25  
26  
27  
28  
29  
30  
31  
32  
33  
34  
35  
36  
37  
38  
39  
40  
41  
42  
43  
44  
45  
46  
47  
48  
49  
50  
51  
52  
53  
54  
55  
56  
57  
58  
59  
60

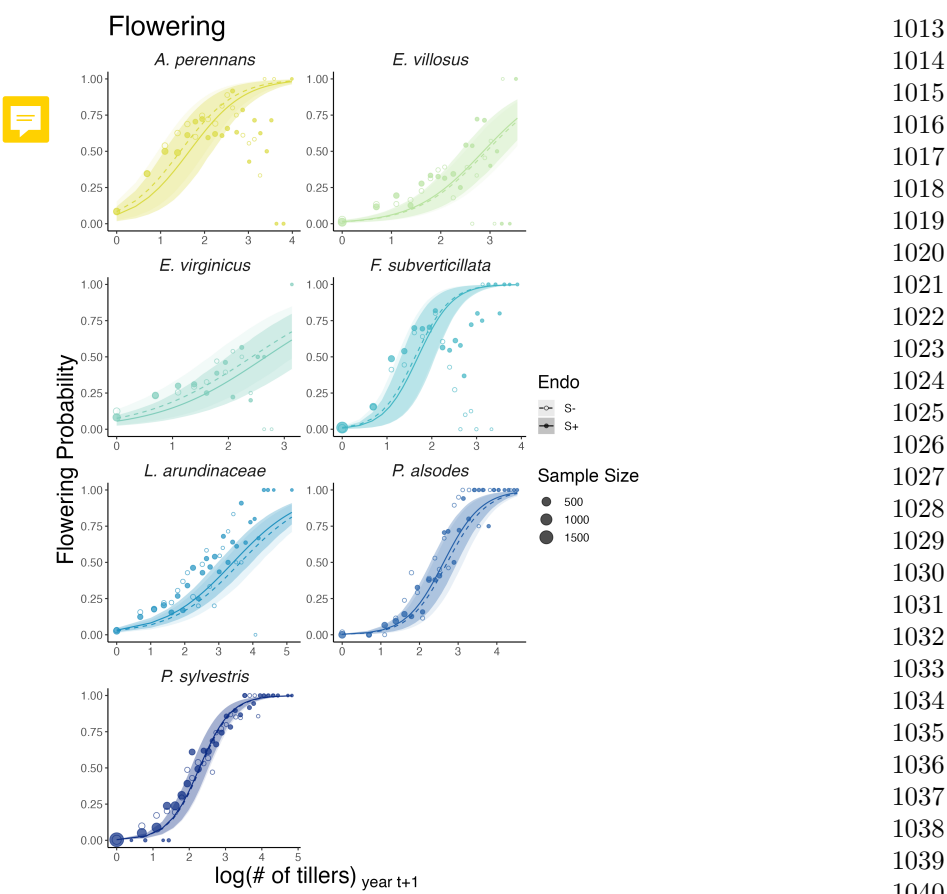
## Supplemental Figures S1-S28



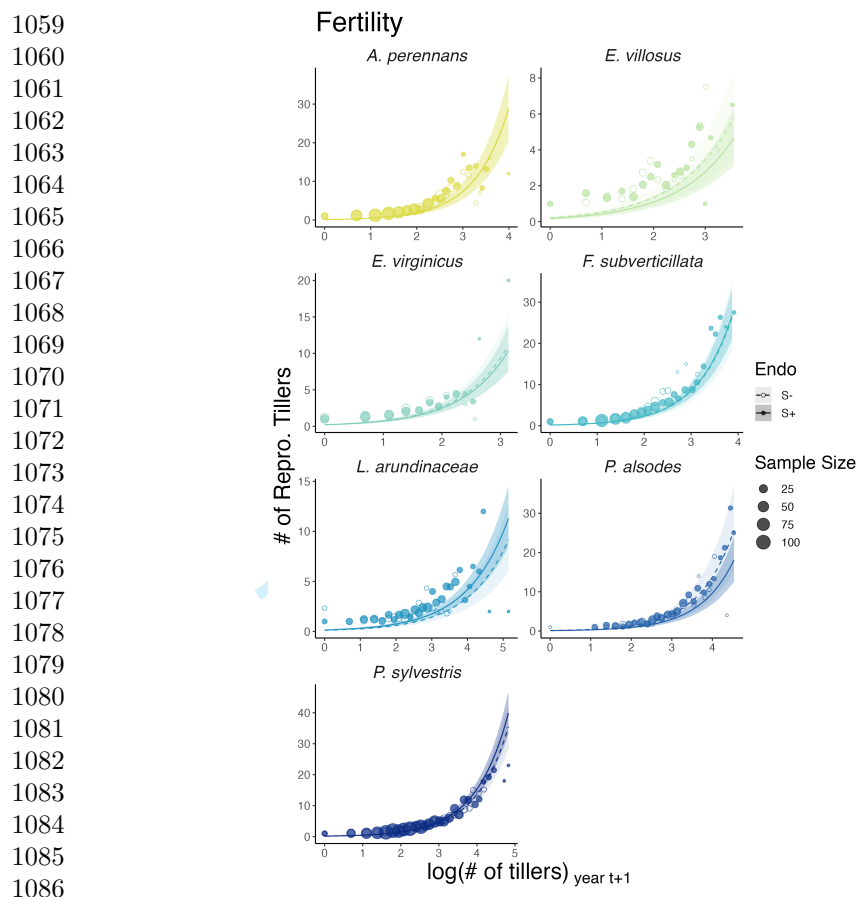
**Fig. S1** Effect of endophyte symbiosis on mean adult survival. Fitted curves represent the size-specific mean survival probability along with data binned by size shown as open circles with a dashed line for symbiont-free (S-) plants, while the solid line and filled circles represent symbiotic (S+) plants. 80% credible intervals are shown with dark shading for S+, or light shading for S-.



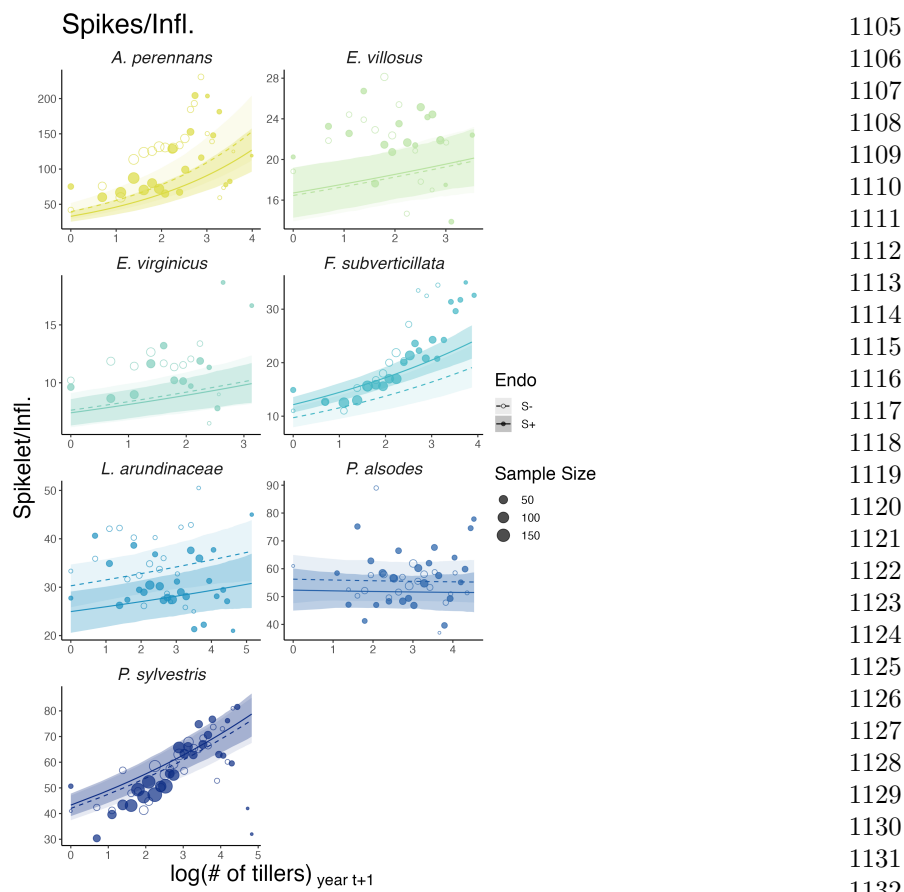
**Fig. S2** Effect of endophyte symbiosis on mean adult growth. Fitted curves represent the size-specific mean expected plant size along with data binned by size shown as open circles with a dashed line for symbiont-free (S-) plants, while the solid line and filled circles represent symbiotic (S+) plants. 80% credible intervals are shown with dark shading for S+, or light shading for S-.



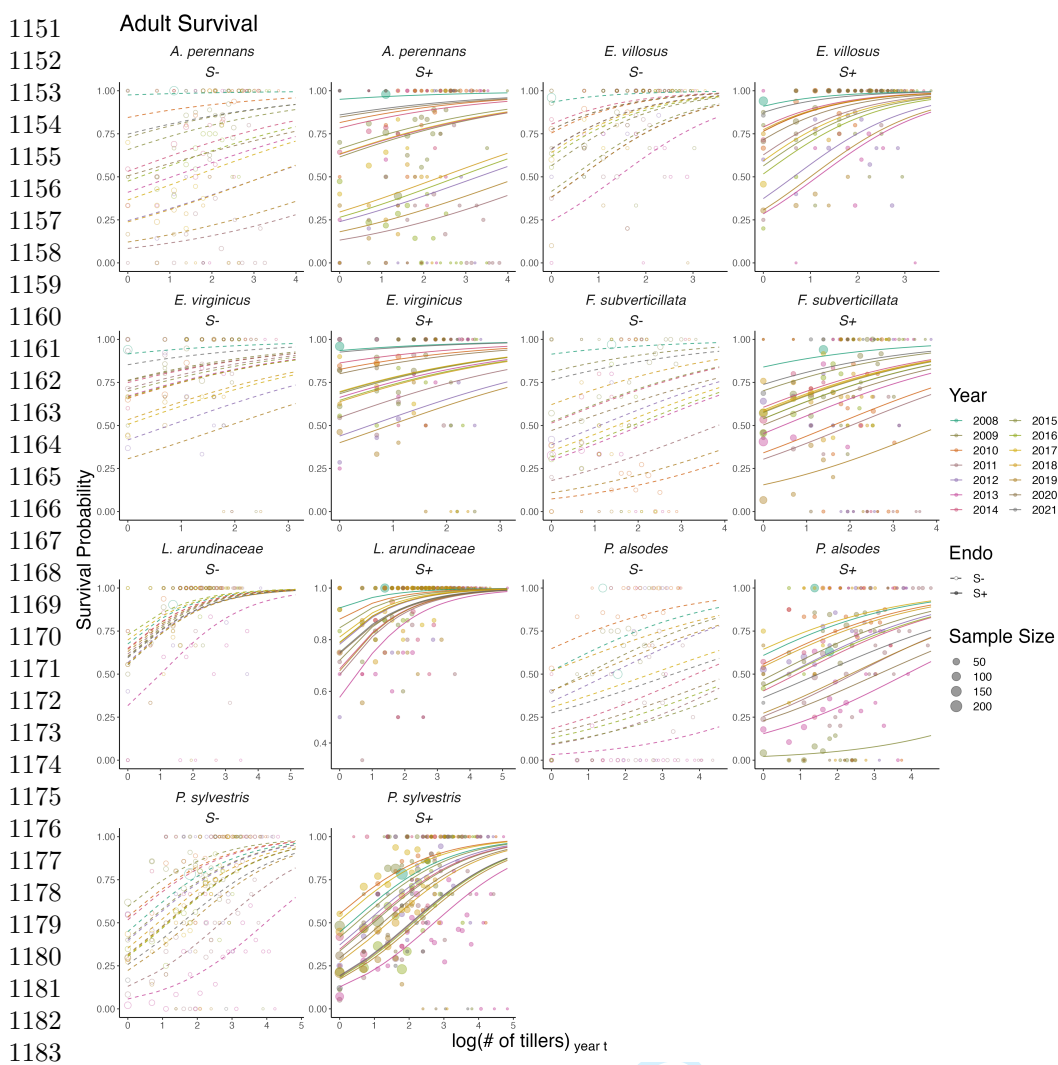
**Fig. S3** Effect of endophyte symbiosis on mean flowering. Fitted curves represent the size-specific mean flowering probability along with data binned by size shown as open circles with a dashed line for symbiont-free (S-) plants, while the solid line and filled circles represent symbiotic (S+) plants. 80% credible intervals are shown with dark shading for S+, or light shading for S-.



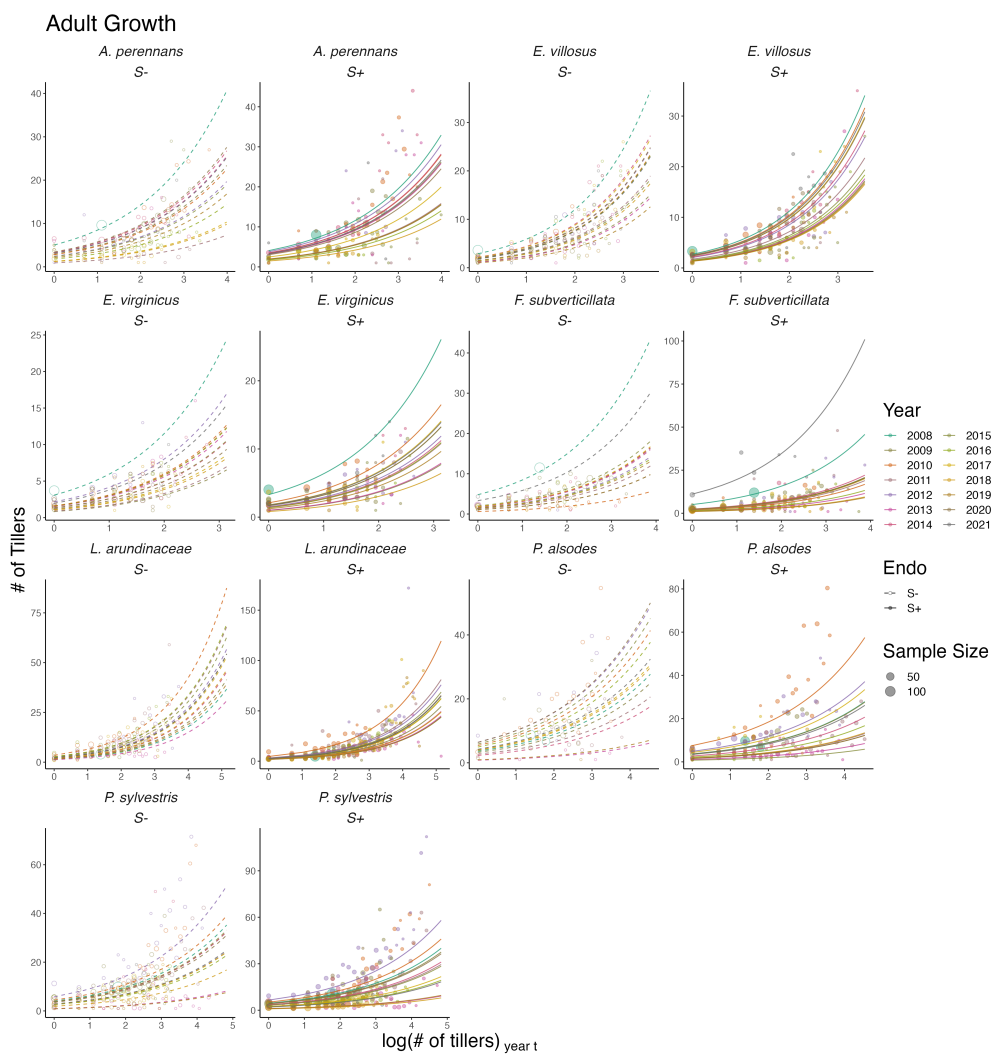
1087 **Fig. S4** Effect of endophyte symbiosis on mean fertility. Fitted curves represent the size-specific  
1088 mean expected number of flowering tillers along with data binned by size shown as open circles with  
1089 a dashed line for symbiont-free (*S-*) plants, while the solid line and filled circles represent symbiotic  
1090 (*S+*) plants. 80% credible intervals are shown with dark shading for *S+*, or light shading for *S-*.



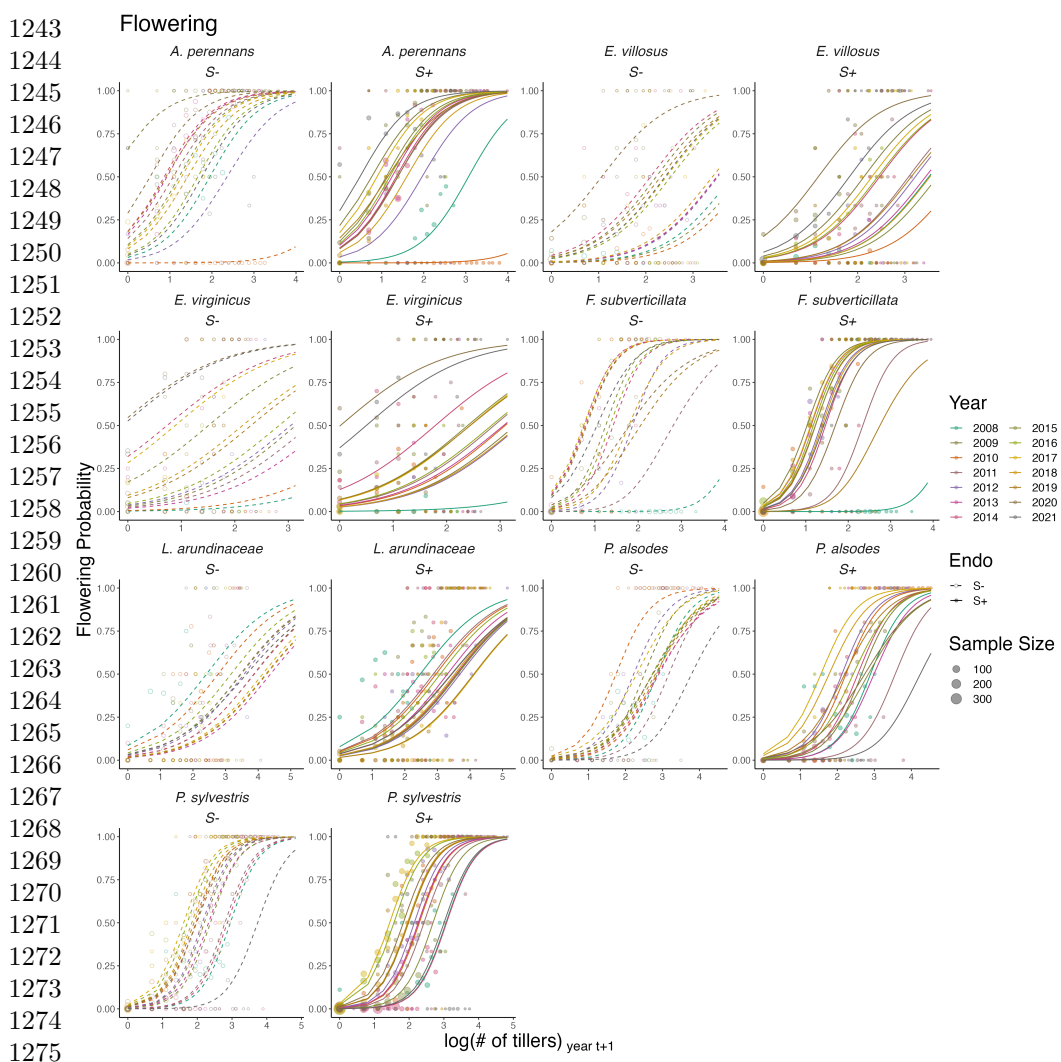
**Fig. S5** Effect of endophyte symbiosis on mean spikelet production. Fitted curves represent the size-specific mean expected number of spikelets per inflorescence along with data binned by size shown as open circles with a dashed line for symbiont-free (S-) plants, while the solid line and filled circles represent symbiotic (S+) plants. 80% credible intervals are shown with dark shading for S+, or light shading for S-.



1185 **Fig. S6** Effect of endophyte symbiosis on yearly adult survival. Fitted curves represent the size-  
1186 specific annual survival probability along with data binned by size and census year shown as open  
1187 circles with a dashed line for symbiont-free (S-) plants, while the solid line and filled circles represent  
1188 symbiotic (S+) plants.



**Fig. S7** Effect of endophyte symbiosis on yearly adult growth. Fitted curves represent the size-specific annual expected plant size along with data binned by size and census year shown as open circles with a dashed line for symbiont-free (S-) plants, while the solid line and filled circles represent symbiotic (S+) plants.



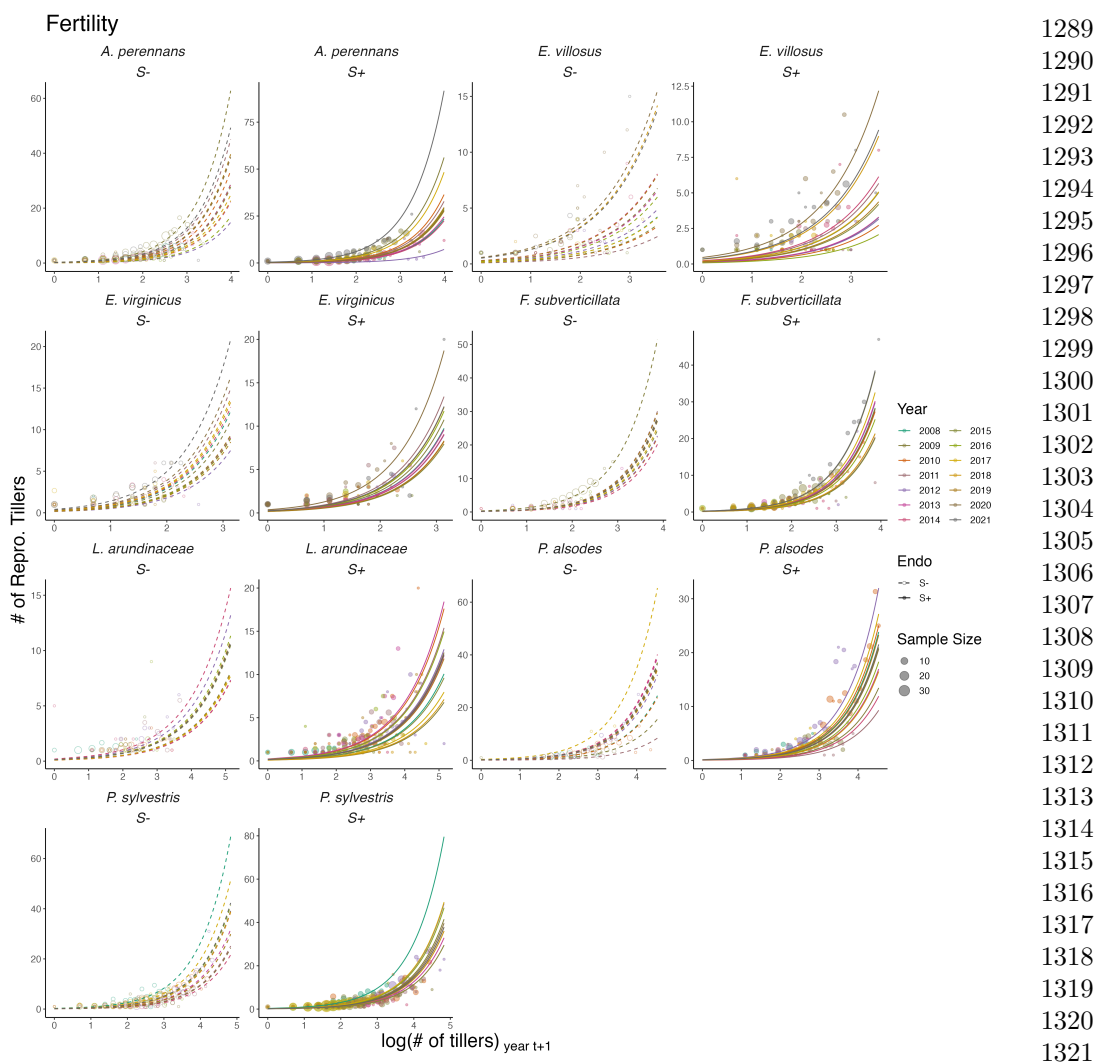
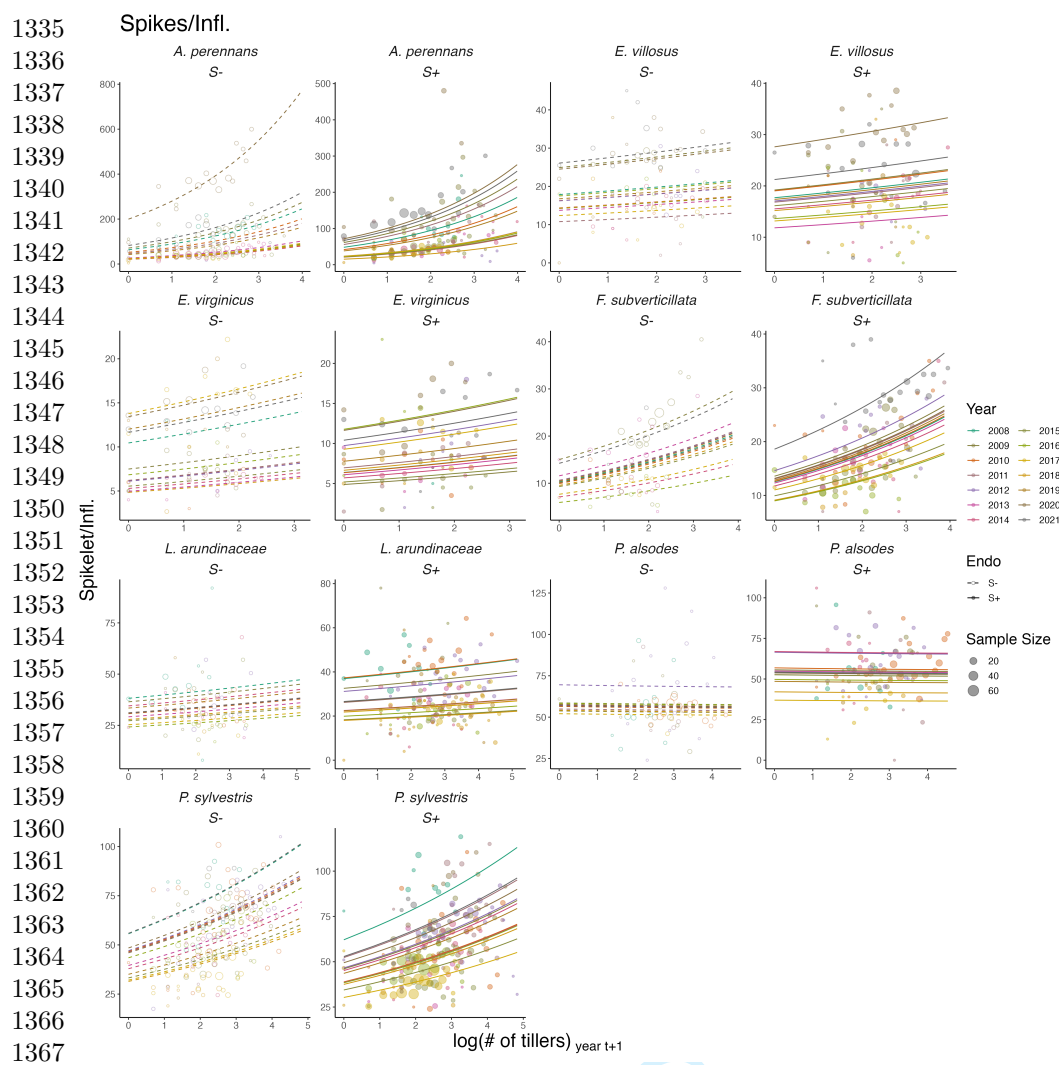


**Fig. S9** Effect of endophyte symbiosis on yearly fertility. Fitted curves represent the size-specific annual expected number of flowering tillers along with data binned by size and census year shown as open circles with a dashed line for symbiont-free (S-) plants, while the solid line and filled circles represent symbiotic (S+) plants.



1369 **Fig. S10** Effect of endophyte symbiosis on yearly spikelet production. Fitted curves represent the  
 1370 size-specific annual expected number of spikelets per inflorescence along with data binned by size and  
 1371 census year shown as open circles with a dashed line for symbiont-free (S-) plants, while the solid line  
 1372 and filled circles represent symbiotic (S+) plants.

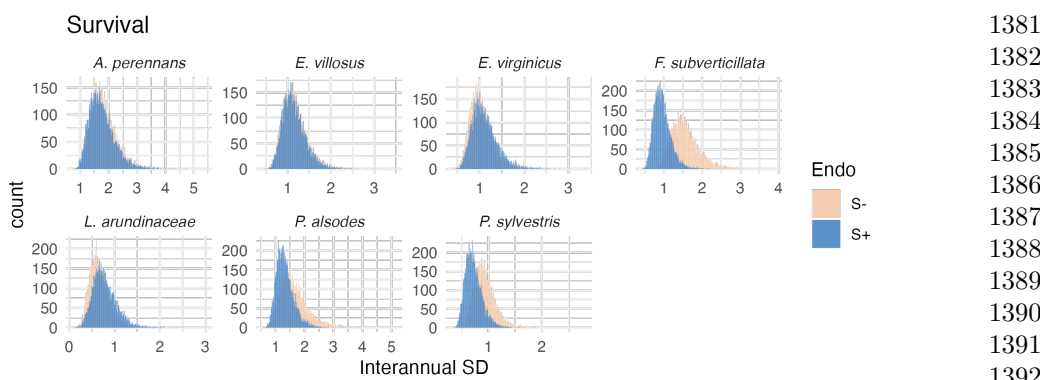


**Fig. S11** Posterior distributions of the standard deviations of inter-annual year effects for survival. Histograms include 7500 post-warmup MCMC samples for symbiotic (S+; blue) and symbiont-free (S-; tan) plants from fitted vital rate model.

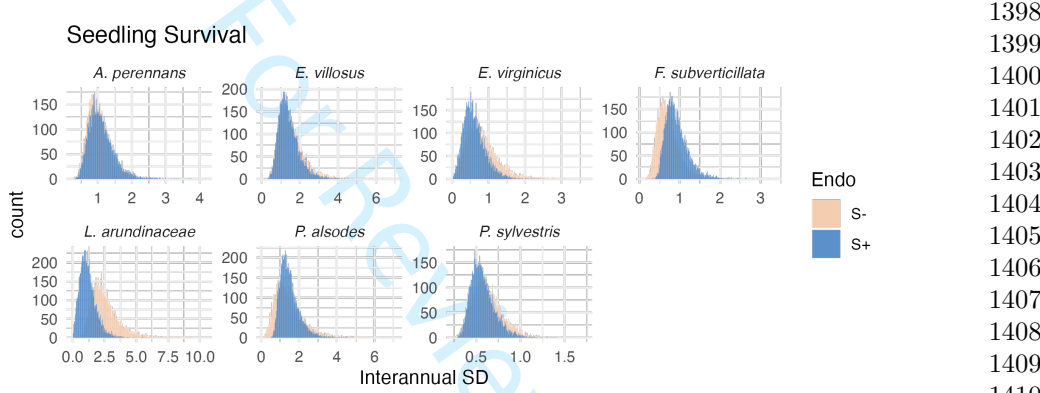
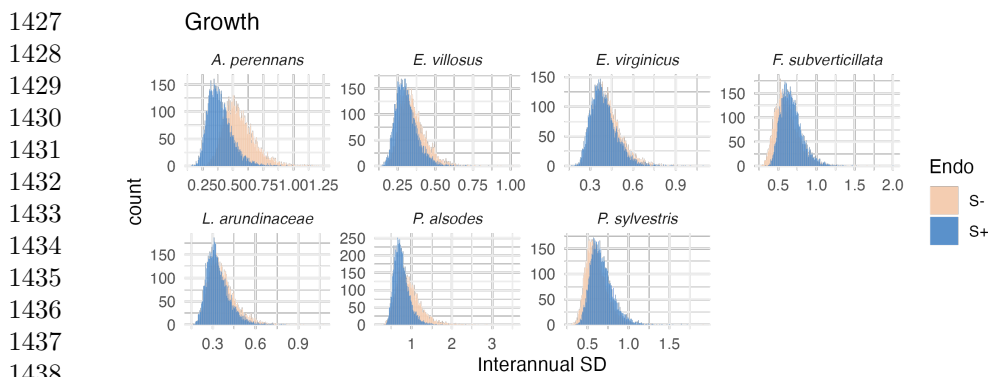
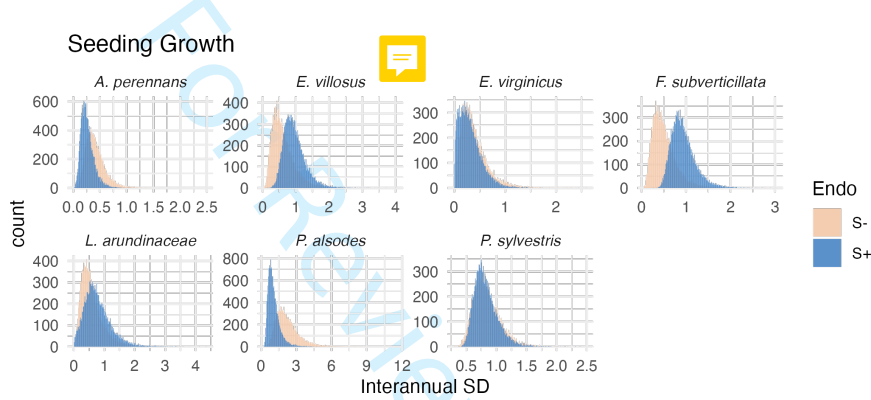


**Fig. S12** Posterior distributions of the standard deviations of inter-annual year effects for seedling survival. Histograms include 7500 post-warmup MCMC samples for symbiotic (S+; blue) and symbiont-free (S-; tan) plants from fitted vital rate model.



1439 **Fig. S13** Posterior distributions of the standard deviations of inter-annual year effects for growth.  
 1440 Histograms include 7500 post-warmup MCMC samples for symbiotic (S+; blue) and symbiont-free  
 1441 (S-; tan) plants from fitted vital rate model.



1457 **Fig. S14** Posterior distributions of the standard deviations of inter-annual year effects for seedling  
 1458 growth. Histograms include 7500 post-warmup MCMC samples for symbiotic (S+; blue) and symbiont-free  
 1459 (S-; tan) plants from fitted vital rate model.

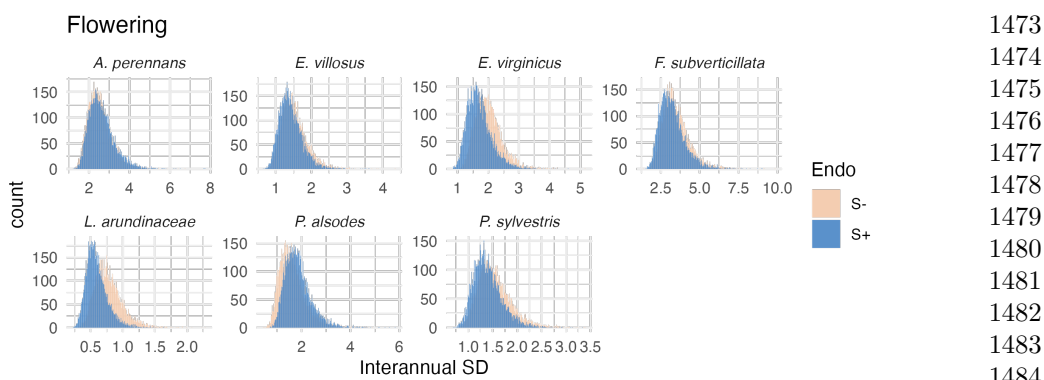


**Fig. S15** Posterior distributions of the standard deviations of inter-annual year effects for flowering probability. Histograms include 7500 post-warmup MCMC samples for symbiotic (S+; blue) and symbiont-free (S-; tan) plants from fitted vital rate model.

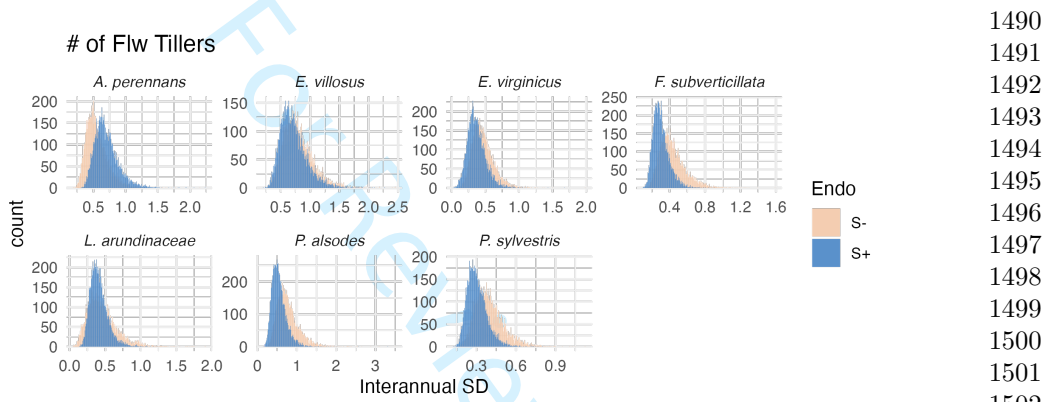
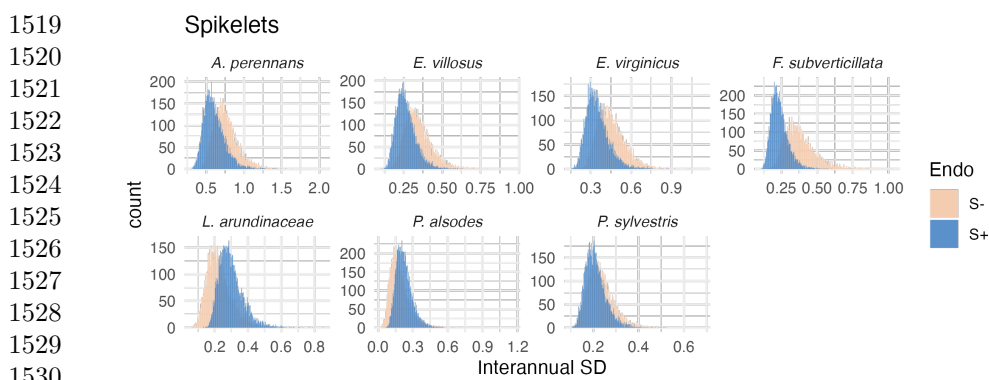
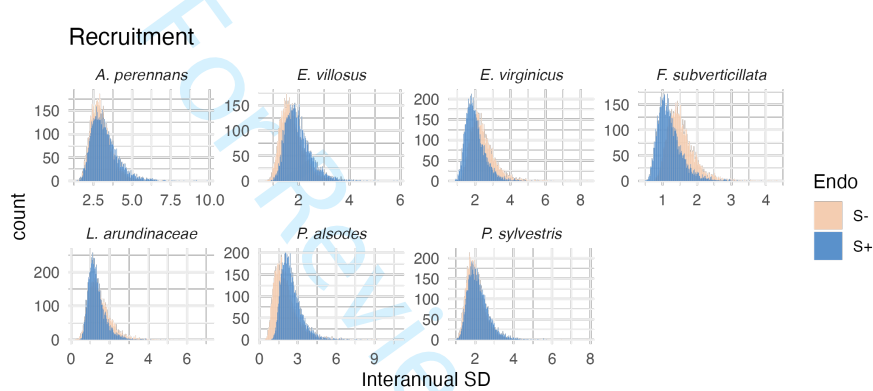


**Fig. S16** Posterior distributions of the standard deviations of inter-annual year effects for fertility (no. of flowering tillers). Histograms include 7500 post-warmup MCMC samples for symbiotic (S+; blue) and symbiont-free (S-; tan) plants from fitted vital rate model.



1531 **Fig. S17** Posterior distributions of the standard deviations of inter-annual year effects for spikelets  
 1532 per inflorescence. Histograms include 7500 post-warmup MCMC samples for symbiotic (S+; blue)  
 1533 and symbiont-free (S-; tan) plants from fitted vital rate model.



1549 **Fig. S18** Posterior distributions of the standard deviations of inter-annual year effects for  
 1550 recruitment. Histograms include 7500 post-warmup MCMC samples for symbiotic (S+; blue) and  
 symbiont-free (S-; tan) plants from fitted vital rate model.

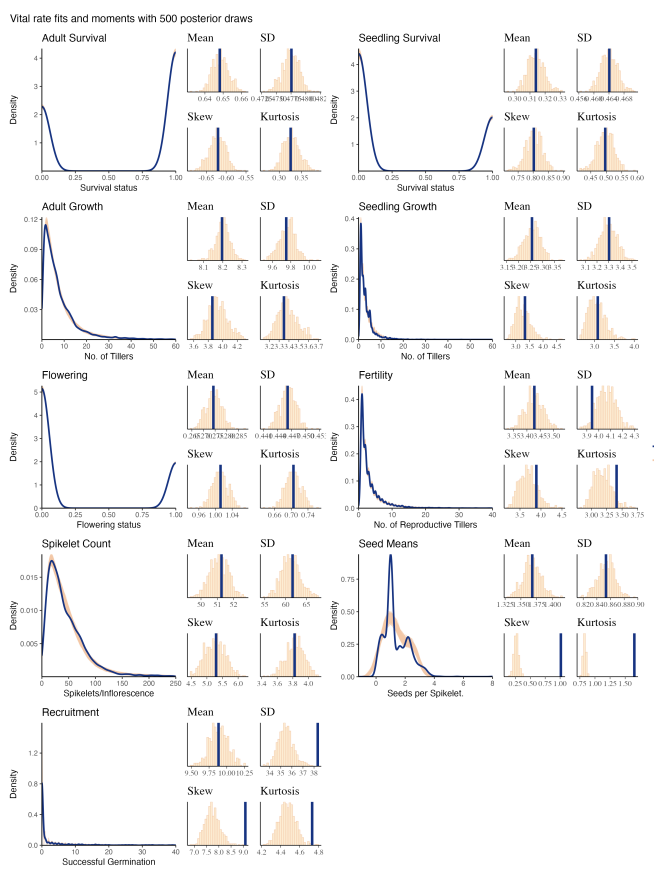
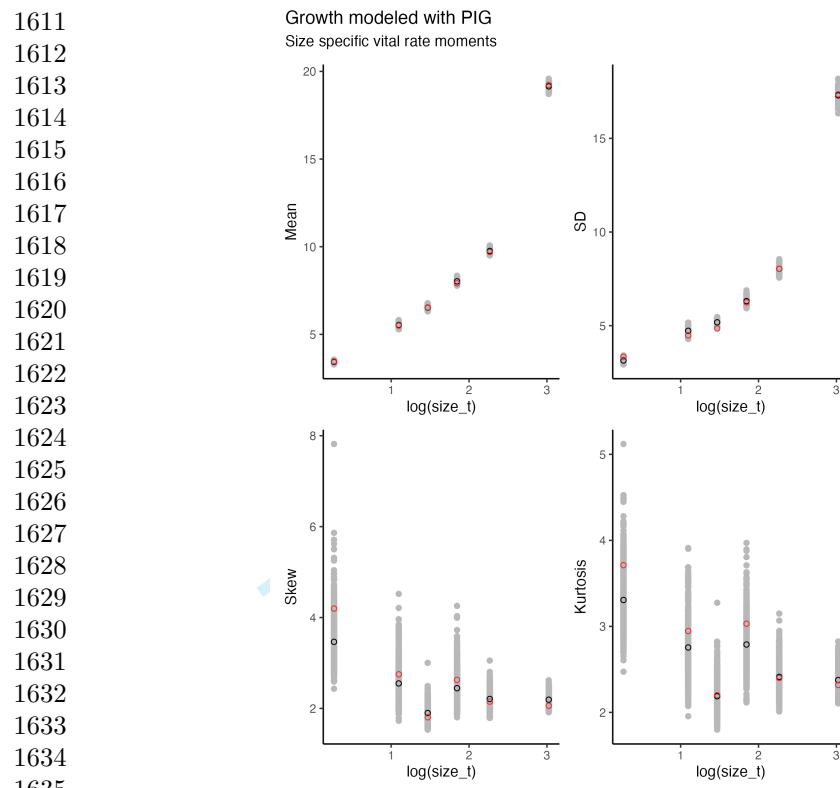


**Fig. S19** Consistency between real data and simulated values indicates that fitted models describe the data well. Graphs show posterior predictive check for statistical models of demographic vital rates. Lines show density distributions of observed data (blue line) compared to data simulated from fitted models (tan lines) generated from 500 draws from posterior distributions of model parameters.



1636 Fig. S20 Consistency between real data and fitted values across sizes indicates that the growth  
1637 model is accurately capturing size dependence. Graphs of posterior predictive check for mean and  
1638 higher moments of the growth model across size. Points show the value of statistical moments binned  
1639 across size for the observed data (red circles) compared to the simulated datasets (grey circles) and  
1640 the median of the simulated values (black circles) generated from 500 posterior draws from the fitted  
1641 model.

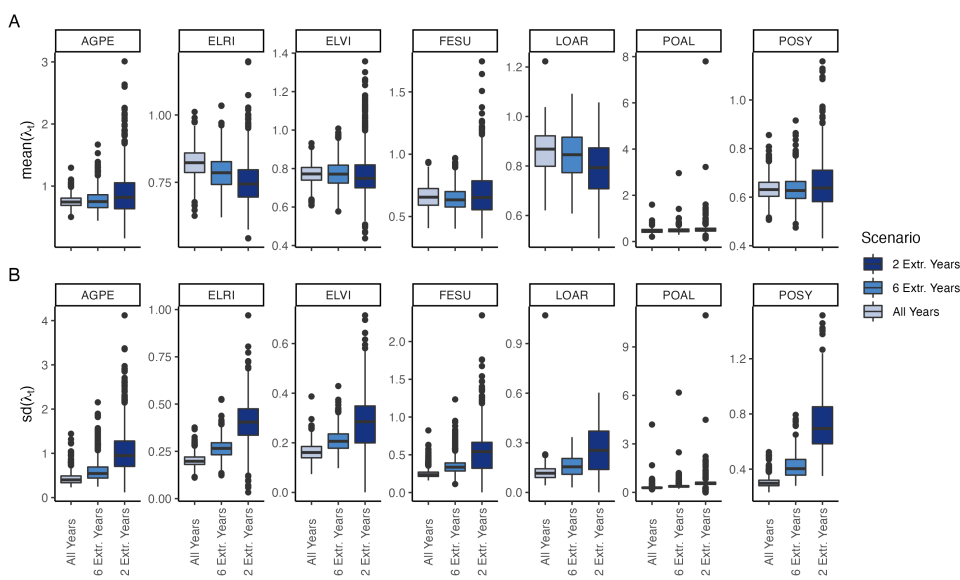


**Fig. S21** (A) Mean and (B) standard deviation of annual growth rate values during simulation scenarios. Each scenario selects from observed transition matrixes, increasing the variance by selecting either all observed years, or a set (6 or 2 years) that have the highest and lowest growth rates for symbiont-free populations.

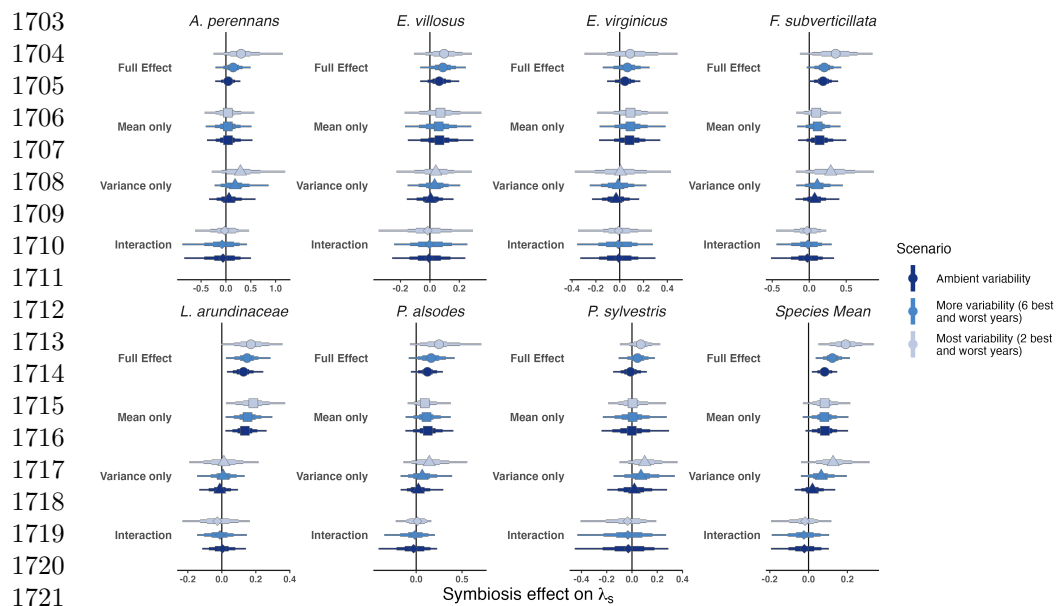


**Fig. S22** Endophyte contributions to stochastic growth rates under observed and elevated variance across species. The total effect of endophytes (circle) comes from mean benefits (square) and variance buffering (triangle) as well as the interaction between mean and variance effects (diamond). Shapes indicate the posterior mean of each contribution, along with bars for the 50, 75 and 95 % credible intervals. Under scenarios of increasing variance, represented by increasing color intensity, effects of variance buffering increase leading to a more mutualistic symbiosis.

1  
2  
3  
4  
5  
6  
7  
8  
9  
10  
11  
12  
13  
14  
15  
16  
17  
18  
19  
20  
21  
22  
23  
24  
25  
26  
27  
28  
29  
30  
31  
32  
33  
34  
35  
36  
37  
38  
39  
40  
41  
42  
43  
44  
45  
46  
47  
48  
49  
50  
51  
52  
53  
54  
55  
56  
57  
58  
59  
60

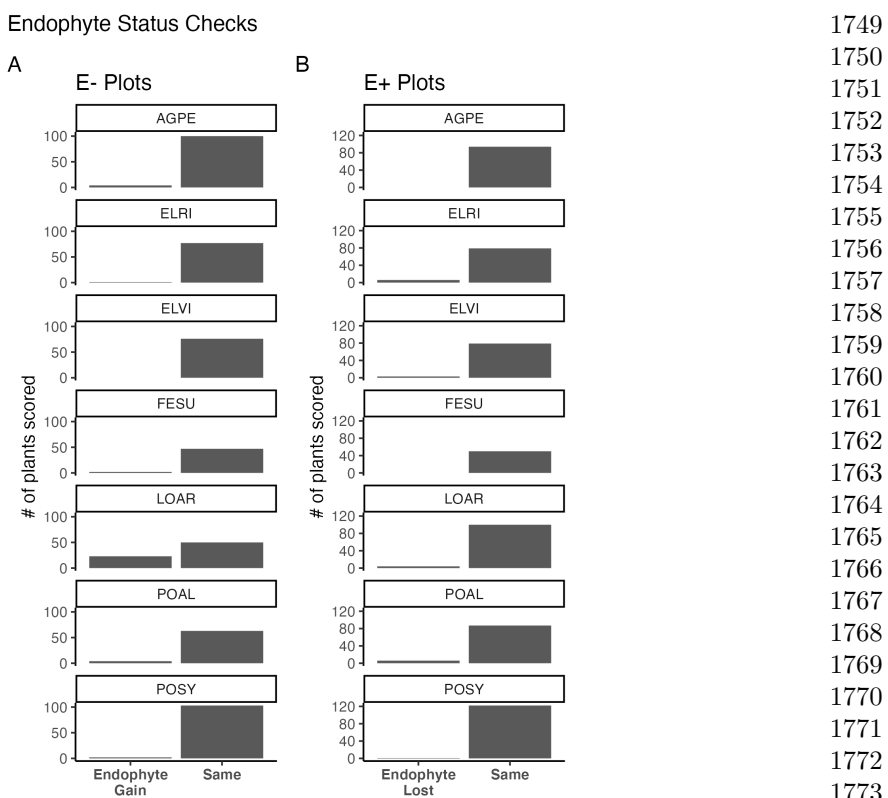


**Fig. S23** Faithfulness of experimental plots to assigned endophyte status. Counts of plants scored with leaf peels or seed squashes to check the faithfulness of recruits to the assigned plot-level endophyte status. (A) Endophytic plants may be gained in initially S- plots, or (B) lost in initially S+ plots.

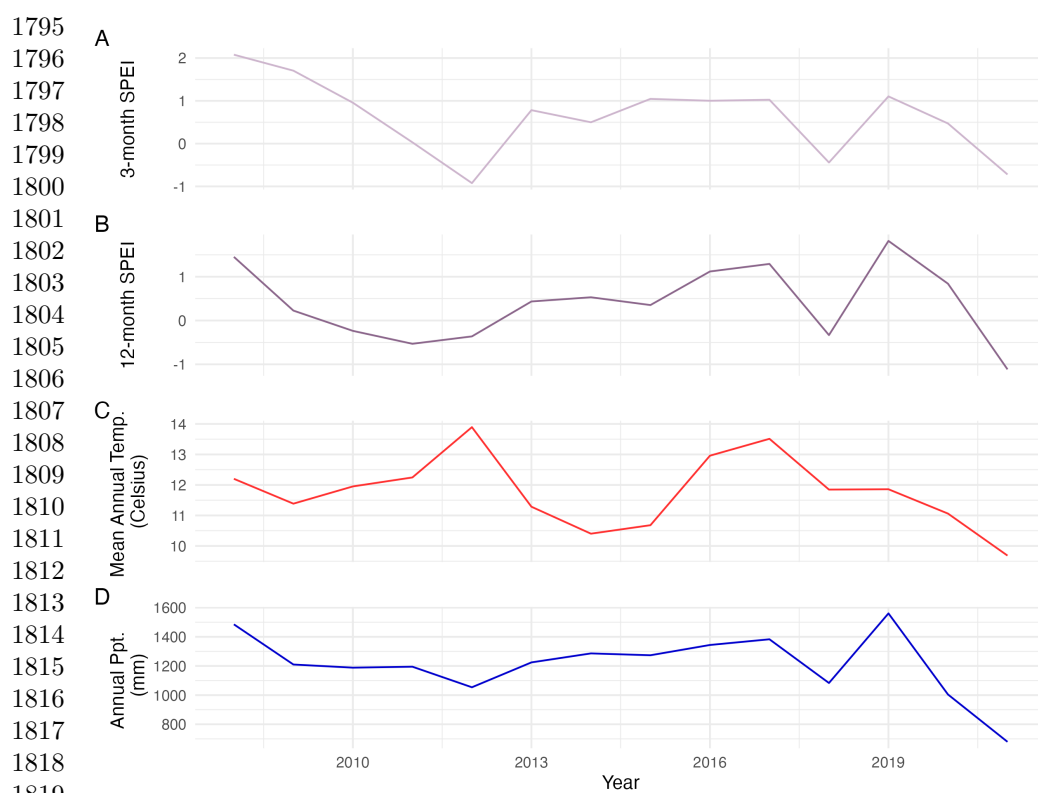


**Fig. S24** Weather station time-series for Bloomington, IN. The Seasonal Precipitation-Evapotranspiration Index (SPEI) calculated for the (A) three month growing season and (B) annually from daily weather station observations of (C) average temperatures and (D) cumulative precipitation. Climatic data shown are determined by the census year centered on the month of July.

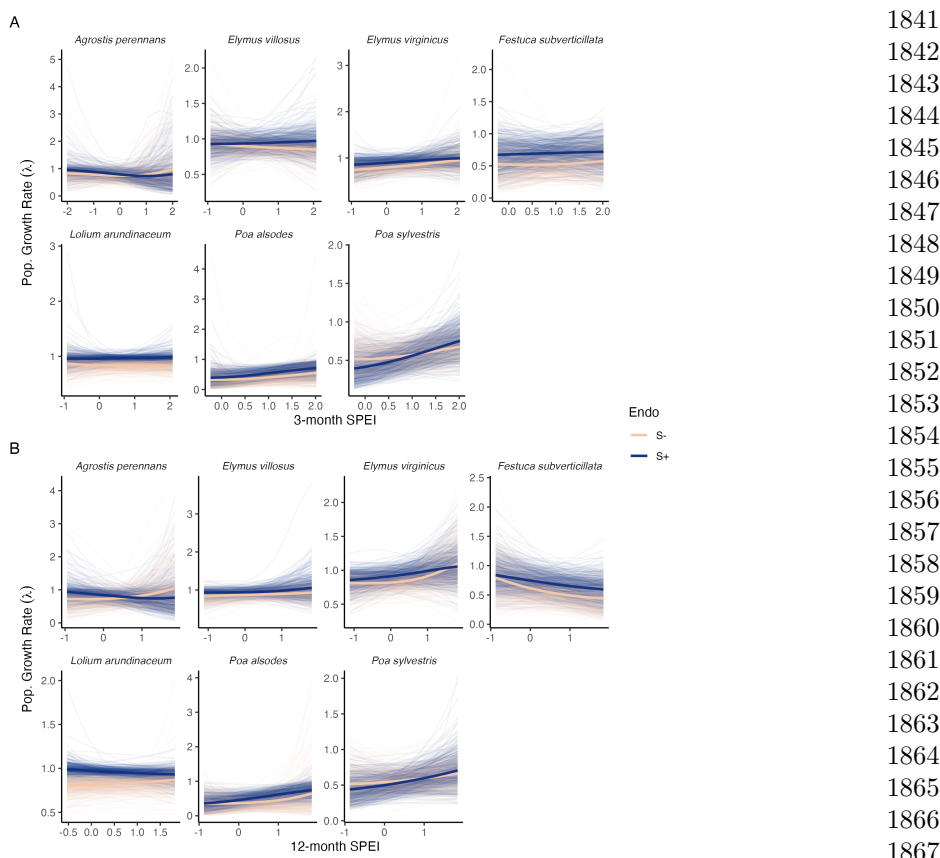


**Fig. S25** Predicted population growth rates across drought indices. Symbiotic (S+; blue) and symbiont-free (S-; tan) populations respond differently to climate as measured by the (A) 3-month SPEI and (B) 12-month SPEI. Thick lines represent the predicted mean growth rate and thin lines show 500 posterior draws.

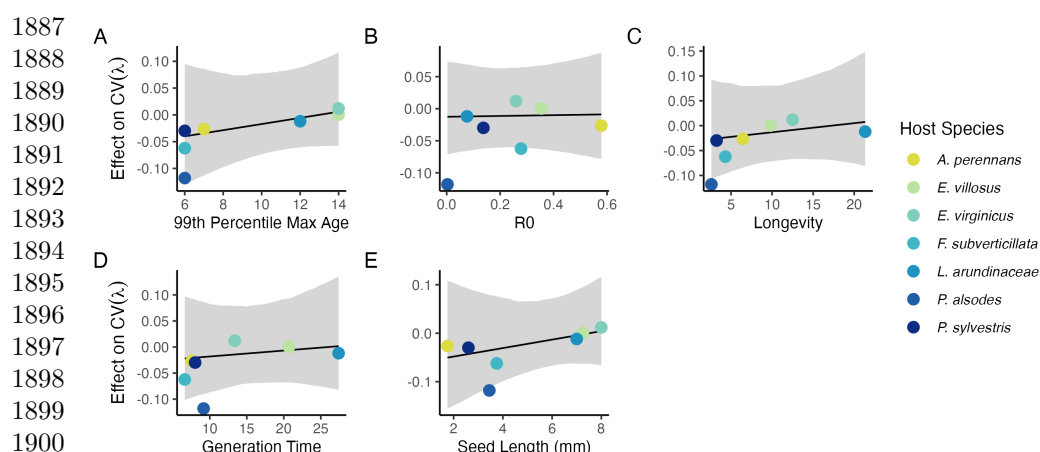


**Fig. S26** Relationship between variance buffering and life history traits describing the fast-slow life history continuum accounting for phylogenetic covariance between grass host species. Regressions between life history traits describing the fast-slow life history continuum ((A) 99th percentile maximum age observed during long term censuses in years; (B) Net reproductive rate; (C) Longevity; (D) Generation time in years; (E) Seed size) and the effect of endophyte symbiosis on the coefficient of variation in population growth rate ( $\lambda$ ). Each panel shows the fitted mean relationship (line) along with the 95% credible interval.

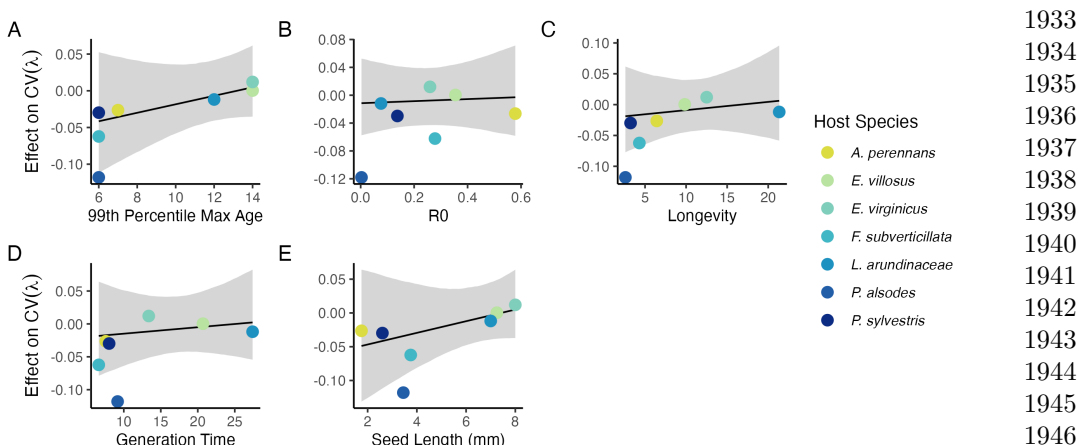


**Fig. S27** Relationship between variance buffering and life history traits describing the fast-slow life history continuum accounting for phylogenetic covariance between *Epichloë* symbionts. Regressions between life history traits describing the fast-slow life history continuum ((A) 99th percentile maximum age observed during long term censuses in years; (B) Net reproductive rate; (C) Longevity; (D) Generation time in years; (E) Seed size) and the effect of endophyte symbiosis on the coefficient of variation in population growth rate ( $\lambda$ ). Results are similar to regressions accounting for host plant phylogeny (Fig. S25), however symbionts are all within a single genus. Each panel shows the fitted mean relationship (line) along with the 95% credible interval.

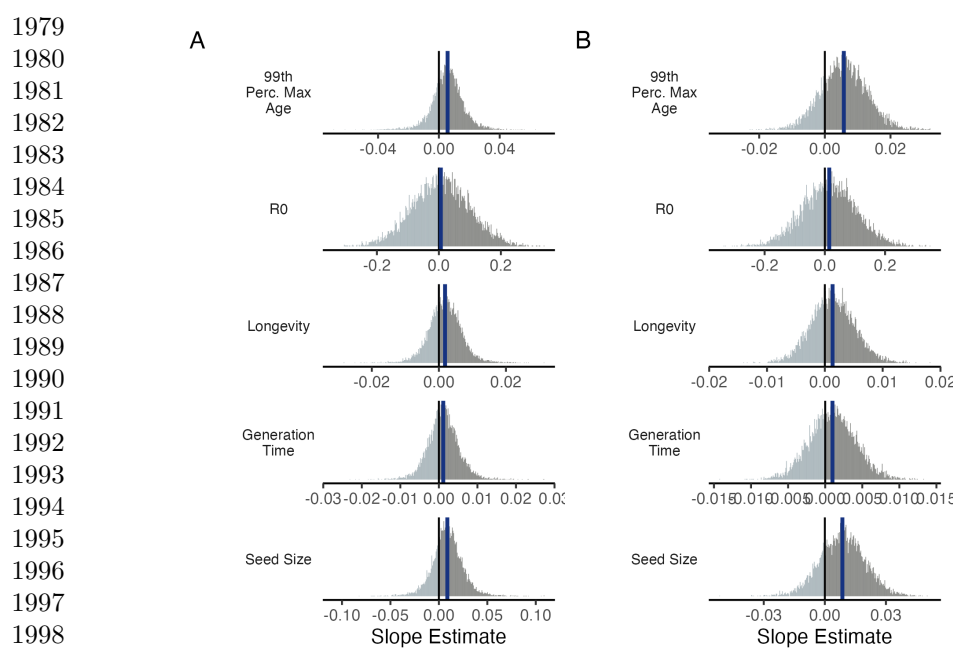


**Fig. S28** Posterior estimates of life history trait effects on variance buffering. Grey histograms show the posterior distribution of the slope parameter from models incorporating (A) host plant phylogenetic covariance and (B) symbiont phylogenetic covariance for each life history trait with blue bars showing the posterior mean.

**Supplemental Tables S1-S3**

2025  
2026  
2027  
2028  
2029  
2030  
2031  
2032  
2033  
2034  
2035  
2036  
2037  
2038  
2039  
2040  
2041  
2042  
2043  
2044  
2045  
2046  
2047  
2048  
2049  
2050  
2051  
2052  
2053  
2054  
2055  
2056  
2057  
2058  
2059  
2060  
2061  
2062  
2063  
2064  
2065  
2066  
2067  
2068  
2069  
2070

1  
2  
3  
4  
5  
6  
7  
8  
9  
10  
11  
12  
13  
14  
15  
16  
17  
18  
19  
20  
21  
22  
23  
24  
25  
26  
27  
28  
29  
30  
31  
32  
33  
34  
35  
36  
37  
38  
39  
40  
41  
42  
43  
44  
45  
46  
47  
48  
49  
50  
51  
52  
53  
54  
55  
56  
57  
58  
59  
60

2071  
2072  
2073  
2074  
2075  
2076  
2077  
2078  
2079  
2080  
2081  
2082  
2083  
2084  
2085  
2086  
2087  
2088  
2089  
2090  
2091  
2092  
2093  
2094  
2095  
2096  
2097  
2098  
2099  
2100  
2101  
2102  
2103  
2104  
2105  
2106  
2107  
2108  
2109  
2110  
2111  
2112  
2113  
2114  
2115  
2116

**Table S1** Summary of host-endophyte propagation and transplant methods

Host Species	Symbiont Species	Heat treatment duration (Temp.)	Transplant date
<i>Agrostis perennans</i>	<i>E. amarillans</i>	12 min. hot water bath (60 °C)	April 2008 (10 plots)
<i>Elymus villosus</i>	<i>E. elymi</i>	6 days drying oven (60 °C)	April 2008 (10 plots)
<i>Elymus virginicus</i>	<i>E. elymi</i> or <i>EviTG-1</i>	6 days drying oven (60 °C)	April 2008 (10 plots)
<i>Festuca subverticillata</i>	<i>E. starrii</i>	6 days drying oven (60 °C)	April 2008 (10 plots)
<i>Lolium arundinaceum</i>	<i>E. coenophiala</i>	6 days drying oven (60 °C)	Sept. 2007 (10 plots)
<i>Poa alsodes</i>	<i>E. alsodes</i>	7 days drying oven (60 °C)	Sept. 2007 (8 plots)/April 2008 (10 plots)
<i>Poa sylvestris</i>	<i>E. PsyTG-1</i>	7 days drying oven (60 °C)	Sept. 2007 (8 plots)/April 2008 (10 plots)

**Table S2** Summary of focal life history traits

Host Species	Observed max age (years)	99th percentile max age (years)	Generation time (years)	$R_0$	Longevity (years)	Seed Length (mm.)	Imperfect transmission rate (%)	Stromata Observed of indiv. per species)
<i>Agrostis perennans</i>	11	7	7.6	0.58	6.4	1.75	69.8	0.0
<i>Elymus villosus</i>	14	14	20.7	0.35	9.8	7.25	100	4.6
<i>Elymus virginicus</i>	14	14	13.4	0.25	12.5	8	100	0.6
<i>Festuca subverticillata</i>	9	6	6.6	0.28	4.3	3.75	42.7	0.0
<i>Lolium arundinaceum</i>	12*	12*	27.4	0.08	21.3	7	100	0.0
<i>Poa alsodes</i>	8	6	9.2	0.003	2.6	3.45	99.9	0.0
<i>Poa sylvestris</i>	12	6	8.0	0.14	3.2	2.6	16.6	0.1

\*Censuses for *L. arundinaceum* plots stopped after year 12 of the experiment.

1  
2  
3  
4  
5  
6  
7  
8  
9  
10  
11  
12  
13  
14  
15  
16  
17  
18  
19  
20  
21  
22  
23  
24  
25  
26  
27  
28  
29  
30  
31  
32  
33  
34  
35  
36  
37  
38  
39  
40  
41  
42  
43  
44  
45  
46  
47  
48  
49  
50  
51  
52  
53  
54  
55  
56  
57  
58  
59  
60

2163  
2164  
2165  
2166  
2167  
2168  
2169  
2170  
2171  
2172  
2173  
2174  
2175  
2176  
2177  
2178  
2179  
2180  
2181  
2182  
2183  
2184  
2185  
2186  
2187  
2188  
2189  
2190  
2191  
2192  
2193  
2194  
2195  
2196  
2197  
2198  
2199  
2200  
2201  
2202  
2203  
2204  
2205  
2206  
2207  
2208

**Table S3** Summary of host-endophyte drought sensitivities

Host Species	Effect on CV( $\lambda$ )	Effect on Mean( $\lambda$ )	$\frac{\Delta\lambda^-}{\Delta SPEI_3}$	$\frac{\Delta\lambda^+}{\Delta SPEI_3}$	3 month S- to S+ ratio	$\frac{\Delta\lambda^-}{\Delta SPEI_{12}}$	$\frac{\Delta\lambda^+}{\Delta SPEI_{12}}$	12 month S- to S+ ratio
<i>Agrostis perennans</i>	-0.0264	0.0441	0.03	-0.04	0.85	0.11	-0.06	1.82
<i>Elymus villosus</i>	0.0003	0.0509	-0.03	0.01	1.95	0.03	0.04	0.70
<i>Elymus virginicus</i>	0.0120	0.0578	0.07	0.05	1.50	0.10	0.07	1.42
<i>Festuca subverticillata</i>	-0.0622	0.1639	0.02	0.02	1.01	-0.13	-0.09	1.43
<i>Lolium arundinaceum</i>	-0.0118	0.1022	-0.01	0.01	1.32	0.03	-0.03	1.02
<i>Poa alsodes</i>	-0.1179	0.1282	0.10	0.14	0.71	0.11	0.14	0.73
<i>Poa sylvestris</i>	-0.0298	-0.0085	0.07	0.16	0.44	0.05	0.10	0.55

- 1  
2  
3  
4  
5  
6  
7  
8  
9  
10  
11  
12  
13  
14  
15  
16  
17  
18  
19  
20  
21  
22  
23  
24  
25  
26  
27  
28  
29  
30  
31  
32  
33  
34  
35  
36  
37  
38  
39  
40  
41  
42  
43  
44  
45  
46  
47  
48  
49  
50  
51  
52  
53  
54  
55  
56  
57  
58  
59  
60
- ## References
- [1] Seneviratne, S. *et al.* *Changes in climate extremes and their impacts on the natural physical environment* (Cambridge University Press, 2012). 2209  
2210  
2211  
2212  
2213  
2214  
2215  
2216  
2217  
2218  
2219  
2220  
2221  
2222  
2223  
2224  
2225  
2226  
2227  
2228  
2229  
2230  
2231  
2232  
2233  
2234  
2235  
2236  
2237  
2238  
2239  
2240  
2241  
2242  
2243  
2244  
2245  
2246  
2247  
2248  
2249  
2250  
2251  
2252  
2253  
2254
  - [2] IPCC. Climate change 2021: The physical science basis (2021). URL <https://www.ipcc.ch/report/ar6/wg1/>. 2209  
2210  
2211  
2212  
2213  
2214  
2215  
2216  
2217  
2218  
2219  
2220  
2221  
2222  
2223  
2224  
2225  
2226  
2227  
2228  
2229  
2230  
2231  
2232  
2233  
2234  
2235  
2236  
2237  
2238  
2239  
2240  
2241  
2242  
2243  
2244  
2245  
2246  
2247  
2248  
2249  
2250  
2251  
2252  
2253  
2254
  - [3] Lewontin, R. C. & Cohen, D. On Population Growth in a Randomly Varying Environment. *Proceedings of the National Academy of Sciences* **62**, 1056–1060 (1969). URL <https://www.pnas.org/content/62/4/1056>. Publisher: National Academy of Sciences Section: Biological Sciences: Zoology. 2209  
2210  
2211  
2212  
2213  
2214  
2215  
2216  
2217  
2218  
2219  
2220  
2221  
2222  
2223  
2224  
2225  
2226  
2227  
2228  
2229  
2230  
2231  
2232  
2233  
2234  
2235  
2236  
2237  
2238  
2239  
2240  
2241  
2242  
2243  
2244  
2245  
2246  
2247  
2248  
2249  
2250  
2251  
2252  
2253  
2254
  - [4] Tuljapurkar, S. D. Population dynamics in variable environments. III. Evolutionary dynamics of r-selection. *Theoretical Population Biology* **21**, 141–165 (1982). URL <http://www.sciencedirect.com/science/article/pii/0040580982900107>. 2209  
2210  
2211  
2212  
2213  
2214  
2215  
2216  
2217  
2218  
2219  
2220  
2221  
2222  
2223  
2224  
2225  
2226  
2227  
2228  
2229  
2230  
2231  
2232  
2233  
2234  
2235  
2236  
2237  
2238  
2239  
2240  
2241  
2242  
2243  
2244  
2245  
2246  
2247  
2248  
2249  
2250  
2251  
2252  
2253  
2254
  - [5] Cohen, J. E. Comparative statics and stochastic dynamics of age-structured populations. *Theoretical population biology* **16**, 159–171 (1979). 2209  
2210  
2211  
2212  
2213  
2214  
2215  
2216  
2217  
2218  
2219  
2220  
2221  
2222  
2223  
2224  
2225  
2226  
2227  
2228  
2229  
2230  
2231  
2232  
2233  
2234  
2235  
2236  
2237  
2238  
2239  
2240  
2241  
2242  
2243  
2244  
2245  
2246  
2247  
2248  
2249  
2250  
2251  
2252  
2253  
2254
  - [6] Tuljapurkar, S. *Population dynamics in variable environments* Vol. 85 (Springer Science & Business Media, 2013). 2209  
2210  
2211  
2212  
2213  
2214  
2215  
2216  
2217  
2218  
2219  
2220  
2221  
2222  
2223  
2224  
2225  
2226  
2227  
2228  
2229  
2230  
2231  
2232  
2233  
2234  
2235  
2236  
2237  
2238  
2239  
2240  
2241  
2242  
2243  
2244  
2245  
2246  
2247  
2248  
2249  
2250  
2251  
2252  
2253  
2254
  - [7] Pfister, C. A. Patterns of variance in stage-structured populations: evolutionary predictions and ecological implications. *Proceedings of the National Academy of Sciences* **95**, 213–218 (1998). 2209  
2210  
2211  
2212  
2213  
2214  
2215  
2216  
2217  
2218  
2219  
2220  
2221  
2222  
2223  
2224  
2225  
2226  
2227  
2228  
2229  
2230  
2231  
2232  
2233  
2234  
2235  
2236  
2237  
2238  
2239  
2240  
2241  
2242  
2243  
2244  
2245  
2246  
2247  
2248  
2249  
2250  
2251  
2252  
2253  
2254
  - [8] Morris, W. F. *et al.* Longevity can buffer plant and animal populations against changing climatic variability. *Ecology* **89**, 19–25 (2008). 2209  
2210  
2211  
2212  
2213  
2214  
2215  
2216  
2217  
2218  
2219  
2220  
2221  
2222  
2223  
2224  
2225  
2226  
2227  
2228  
2229  
2230  
2231  
2232  
2233  
2234  
2235  
2236  
2237  
2238  
2239  
2240  
2241  
2242  
2243  
2244  
2245  
2246  
2247  
2248  
2249  
2250  
2251  
2252  
2253  
2254
  - [9] Compagnoni, A. *et al.* The effect of demographic correlations on the stochastic population dynamics of perennial plants. *Ecological Monographs* **86**, 480–494 (2016). 2209  
2210  
2211  
2212  
2213  
2214  
2215  
2216  
2217  
2218  
2219  
2220  
2221  
2222  
2223  
2224  
2225  
2226  
2227  
2228  
2229  
2230  
2231  
2232  
2233  
2234  
2235  
2236  
2237  
2238  
2239  
2240  
2241  
2242  
2243  
2244  
2245  
2246  
2247  
2248  
2249  
2250  
2251  
2252  
2253  
2254
  - [10] Ellis, M. M. & Crone, E. E. The role of transient dynamics in stochastic population growth for nine perennial plants. *Ecology* **94**, 1681–1686 (2013). 2209  
2210  
2211  
2212  
2213  
2214  
2215  
2216  
2217  
2218  
2219  
2220  
2221  
2222  
2223  
2224  
2225  
2226  
2227  
2228  
2229  
2230  
2231  
2232  
2233  
2234  
2235  
2236  
2237  
2238  
2239  
2240  
2241  
2242  
2243  
2244  
2245  
2246  
2247  
2248  
2249  
2250  
2251  
2252  
2253  
2254
  - [11] Rodríguez-Caro, R. C. *et al.* The limits of demographic buffering in coping with environmental variation. *Oikos* **130**, 1346–1358 (2021). 2209  
2210  
2211  
2212  
2213  
2214  
2215  
2216  
2217  
2218  
2219  
2220  
2221  
2222  
2223  
2224  
2225  
2226  
2227  
2228  
2229  
2230  
2231  
2232  
2233  
2234  
2235  
2236  
2237  
2238  
2239  
2240  
2241  
2242  
2243  
2244  
2245  
2246  
2247  
2248  
2249  
2250  
2251  
2252  
2253  
2254
  - [12] Tuljapurkar, S. & Orzack, S. H. Population dynamics in variable environments i. long-run growth rates and extinction. *Theoretical Population Biology* **18**, 314–342 (1980). 2209  
2210  
2211  
2212  
2213  
2214  
2215  
2216  
2217  
2218  
2219  
2220  
2221  
2222  
2223  
2224  
2225  
2226  
2227  
2228  
2229  
2230  
2231  
2232  
2233  
2234  
2235  
2236  
2237  
2238  
2239  
2240  
2241  
2242  
2243  
2244  
2245  
2246  
2247  
2248  
2249  
2250  
2251  
2252  
2253  
2254
  - [13] Fieberg, J. & Ellner, S. P. Stochastic matrix models for conservation and management: a comparative review of methods. *Ecology letters* **4**, 244–266 (2001). 2209  
2210  
2211  
2212  
2213  
2214  
2215  
2216  
2217  
2218  
2219  
2220  
2221  
2222  
2223  
2224  
2225  
2226  
2227  
2228  
2229  
2230  
2231  
2232  
2233  
2234  
2235  
2236  
2237  
2238  
2239  
2240  
2241  
2242  
2243  
2244  
2245  
2246  
2247  
2248  
2249  
2250  
2251  
2252  
2253  
2254

- 1  
2  
3 2255 [14] Menges, E. S. Applications of population viability analyses in plant conservation.  
4 2256     *Ecological Bulletins* 73–84 (2000).  
5 2257  
6 2258 [15] Kuparinen, A., Boit, A., Valdovinos, F. S., Lassaux, H. & Martinez, N. D.  
7 2259     Fishing-induced life-history changes degrade and destabilize harvested ecosystems.  
8 2260     *Scientific reports* **6**, 22245 (2016).  
9 2261  
10 2262 [16] Hilde, C. H. *et al.* The Demographic Buffering Hypothesis: Evidence and Chal-  
11 lengeres. *Trends in Ecology & Evolution* **0** (2020). URL [https://www.cell.com/trends/ecology-evolution/abstract/S0169-5347\(20\)30050-1](https://www.cell.com/trends/ecology-evolution/abstract/S0169-5347(20)30050-1). Publisher: Elsevier.  
12  
13 2265 [17] Rodriguez, R., White Jr, J., Arnold, A. E. & Redman, a. R. a. Fungal endophytes:  
14 2266     diversity and functional roles. *New phytologist* **182**, 314–330 (2009).  
15 2267  
16 2268 [18] McFall-Ngai, M. *et al.* Animals in a bacterial world, a new imperative for the  
17 2269     life sciences. *Proceedings of the National Academy of Sciences* **110**, 3229–3236  
18 2270 (2013).  
19 2271  
20 2272 [19] Funkhouser, L. J. & Bordenstein, S. R. Mom knows best: the universality of  
21 2273     maternal microbial transmission. *PLoS biology* **11**, e1001631 (2013).  
22 2274  
23 2275 [20] Fine, P. E. Vectors and vertical transmission: an epidemiologic perspective.  
24 2276     *Annals of the New York Academy of Sciences* **266**, 173–194 (1975).  
25 2277  
26 2278 [21] Russell, J. A. & Moran, N. A. Costs and benefits of symbiont infection in aphids:  
27 2279     variation among symbionts and across temperatures. *Proceedings of the Royal  
28 2280     Society B: Biological Sciences* **273**, 603–610 (2006).  
29  
30 2281 [22] Kivlin, S. N., Emery, S. M. & Rudgers, J. A. Fungal symbionts alter plant  
31 2282     responses to global change. *American Journal of Botany* **100**, 1445–1457 (2013).  
32  
33 2284 [23] Dunbar, H. E., Wilson, A. C. C., Ferguson, N. R. & Moran, N. A. Aphid thermal  
34 2285     tolerance is governed by a point mutation in bacterial symbionts. *PLoS biology*  
35 2286     **5**, e96 (2007).  
36  
37 2288 [24] Reyna, R., Cooke, P., Grum, D., Cook, D. & Creamer, R. Detection and local-  
38 2289     ization of the endophyte *undifilum oxytropis* in locoweed tissues. *Botany* **90**,  
39 2290     1229–1236 (2012).  
40  
41 2292 [25] Saikkonen, K., Gundel, P. E. & Helander, M. Chemical ecology mediated by  
42 2293     fungal endophytes in grasses. *Journal of chemical ecology* **39**, 962–968 (2013).  
43  
44 2295 [26] Neyaz, M., Gardner, D. R., Creamer, R. & Cook, D. Localization of the  
45 2296     swainsonine-producing chaetothyriales symbiont in the seed and shoot apical  
46 2297     meristem in its host *ipomoea carnea*. *Microorganisms* **10**, 545 (2022).  
47  
48 2299 [27] Chamberlain, S. A., Bronstein, J. L. & Rudgers, J. A. How context dependent  
49 2300     are species interactions? *Ecology letters* **17**, 881–890 (2014).

- 1  
2  
3 [28] Jordano, P. Spatial and temporal variation in the avian-frugivore assemblage of prunus mahaleb: patterns and consequences. *Oikos* **479–491** (1994). 2301  
4 2302  
5 2303  
6 [29] Leuchtmann, A. Systematics, distribution, and host specificity of grass endophytes. *Natural toxins* **1**, 150–162 (1992). 2304  
7 2305  
8 [30] Cheplick, G. P., Faeth, S. & Faeth, S. H. *Ecology and evolution of the grass-endophyte symbiosis* (OUP USA, 2009). 2306  
9 2307  
10 2308  
11 [31] Brem, D. & Leuchtmann, A. Epichloë grass endophytes increase herbivore resistance in the woodland grass brachypodium sylvaticum. *Oecologia* **126**, 522–530 (2001). 2309  
12 2310  
13 2311  
14 2312  
15 [32] Decunta, F. A., Pérez, L. I., Malinowski, D. P., Molina-Montenegro, M. A. & Gundel, P. E. A systematic review on the effects of epichloë fungal endophytes on drought tolerance in cool-season grasses. *Frontiers in plant science* **12**, 644731 (2021). 2313  
16 2314  
17 2315  
18 2316  
19 2317  
20 [33] Bacon, C. W. & White, J. F. in *Stains, media, and procedures for analyzing endophytes* 47–56 (CRC Press, 2018). 2318  
21 2319  
22 2320  
23 [34] Rudgers, J. A. & Swafford, A. L. Benefits of a fungal endophyte in elymus virginicus decline under drought stress. *Basic and Applied Ecology* **10**, 43–51 (2009). 2321  
24 2322  
25 2323  
26 2324  
27 [35] Bultman, T. L., White Jr, J. F., Bowdish, T. I., Welch, A. M. & Johnston, J. Mutualistic transfer of epichloë spermatia by phorbis flies. *Mycologia* **87**, 182–189 (1995). 2325  
28 2326  
29 2327  
30 2328  
31 [36] Stan Development Team. RStan: the R interface to Stan (2022). URL <https://mc-stan.org/>. R package version 2.21.7. 2329  
32 2330  
33 [37] Elderd, B. D. & Miller, T. E. Quantifying demographic uncertainty: Bayesian methods for integral projection models. *Ecological Monographs* **86**, 125–144 (2016). 2331  
34 2332  
35 2333  
36 2334  
37 [38] Gabry, J., Simpson, D., Vehtari, A., Betancourt, M. & Gelman, A. Visualization in bayesian workflow. *Journal of the Royal Statistical Society Series A: Statistics in Society* **182**, 389–402 (2019). 2335  
38 2336  
39 2337  
40 2338  
41 [39] Brooks, S. P. & Gelman, A. General methods for monitoring convergence of iterative simulations. *Journal of computational and graphical statistics* **7**, 434–455 (1998). 2339  
42 2340  
43 2341  
44 2342  
45 [40] Gelman, A. & Hill, J. *Data analysis using regression and multilevel/hierarchical models* (Cambridge university press, 2006). 2343  
46 2344  
47 2345  
48 2346  
49  
50  
51 51  
52  
53  
54  
55  
56  
57  
58  
59  
60

- 1  
2  
3 2347 [41] Williams, J. L., Miller, T. E. & Ellner, S. P. Avoiding unintentional eviction from  
4 integral projection models. *Ecology* **93**, 2008–2014 (2012).  
5 2349  
6 2350 [42] Jones, O. R. *et al.* Recompadre and rage—two r packages to facilitate the use of  
7 the compadre and comadre databases and calculation of life-history traits from  
8 matrix population models. *Methods in Ecology and Evolution* **13**, 770–781 (2022).  
9 2353  
10 2354 [43] Flora of North America Editorial Committee Poaceae. *Flora of North America*  
11 *North of Mexico [Online]* **24**, <http://floranorthamerica.org/Poaceae> (1993+). .  
12 2355  
13 2356 [44] Bürkner, P.-C. brms: An R package for Bayesian multilevel models using Stan.  
14 2357 *Journal of Statistical Software* **80**, 1–28 (2017).  
15 2358  
16 2359 [45] Zanne, A. E. *et al.* Three keys to the radiation of angiosperms into freezing  
17 environments. *Nature* **506**, 89–92 (2014).  
18 2361  
19 2362 [46] Leuchtmann, A., Bacon, C. W., Schardl, C. L., White Jr, J. F. & Tadic, M. Nomenclatural  
20 realignment of neotyphodium species with genus epichloë.  
21 *Mycologia* **106**, 202–215 (2014).  
22 2365  
23 2366 [47] Metcalf, C. J. E. *et al.* Statistical modelling of annual variation for inference  
24 on stochastic population dynamics using integral projection models. *Methods in*  
25 *Ecology and Evolution* **6**, 1007–1017 (2015).  
26 2369  
27 2370 [48] Caswell, H. Matrix population models: Construction, analysis, and interpretation.  
28 2nd edn sinauer associates. Inc., Sunderland, MA (2001).  
29 2372  
30 2373 [49] Rees, M. & Ellner, S. P. Integral projection models for populations in temporally  
31 varying environments. *Ecological Monographs* **79**, 575–594 (2009).  
32 2375  
33 2376 [50] Vicente-Serrano, S. M., Beguería, S. & López-Moreno, J. I. A multiscalar drought  
34 index sensitive to global warming: the standardized precipitation evapotranspi-  
35 ration index. *Journal of climate* **23**, 1696–1718 (2010).  
36 2378  
37 2379 [51] Rudgers, J. A. & Clay, K. An invasive plant–fungal mutualism reduces arthropod  
38 diversity. *Ecology Letters* **11**, 831–840 (2008).  
39 2381  
40 2382 [52] Crawford, K. M., Land, J. M. & Rudgers, J. A. Fungal endophytes of native  
41 grasses decrease insect herbivore preference and performance. *Oecologia* **164**,  
42 431–444 (2010).  
43 2385  
44 2386 [53] Murphy, G. I. Pattern in life history and the environment. *The American*  
45 *Naturalist* **102**, 391–403 (1968).  
46 2388  
47 2389 [54] Compagnoni, A. *et al.* Herbaceous perennial plants with short generation time  
48 have stronger responses to climate anomalies than those with longer generation  
49 time. *Nature communications* **12**, 1–8 (2021).  
50 2392  
51  
52  
53  
54  
55  
56  
57  
58  
59  
60

- 1  
2  
3 [55] Le Coeur, C., Yoccoz, N. G., Salguero-Gómez, R. & Vindenes, Y. Life his- 2393  
4 tory adaptations to fluctuating environments: Combined effects of demographic 2394  
5 buffering and lability. *Ecology Letters* **25**, 2107–2119 (2022). 2395  
6  
7 [56] Rees, M. Evolutionary ecology of seed dormancy and seed size. *Philosophical 2396  
8 Transactions of the Royal Society of London. Series B: Biological Sciences* **351**, 2397  
9 1299–1308 (1996). 2398  
10  
11 [57] Moles, A. T. & Westoby, M. Seedling survival and seed size: a synthesis of the 2399  
12 literature. *Journal of Ecology* **92**, 372–383 (2004). 2400  
13  
14 [58] Afkhami, M. E. & Rudgers, J. A. Symbiosis lost: imperfect vertical transmission 2401  
15 of fungal endophytes in grasses. *The American Naturalist* **172**, 405–416 (2008). 2402  
16  
17 [59] Jeschke, J. M. & Kokko, H. The roles of body size and phylogeny in fast and 2403  
18 slow life histories. *Evolutionary Ecology* **23**, 867–878 (2009). 2404  
19  
20 [60] Afkhami, M. E. & Strauss, S. Y. Native fungal endophytes suppress an exotic 2405  
21 dominant and increase plant diversity over small and large spatial scales. *Ecology* 2406  
22 **97**, 1159–1169 (2016). 2407  
23  
24 [61] Smith, E., Vaughan, G., Ketchum, R., McParland, D. & Burt, J. Symbiont 2408  
25 community stability through severe coral bleaching in a thermally extreme lagoon. 2409  
26 *Scientific Reports* **7**, 2428 (2017). 2410  
27  
28 [62] Dallas, J. W. & Warne, R. W. Captivity and animal microbiomes: potential roles 2411  
29 of microbiota for influencing animal conservation. *Microbial Ecology* 1–19 (2022). 2412  
30  
31 [63] Wu, L. *et al.* Reduction of microbial diversity in grassland soil is driven by 2413  
32 long-term climate warming. *Nature Microbiology* **7**, 1054–1062 (2022). 2414  
33  
34 [64] Ehrlén, J. & Morris, W. F. Predicting changes in the distribution and abundance 2415  
35 of species under environmental change. *Ecology letters* **18**, 303–314 (2015). 2416  
36  
37 [65] Chamberlain, S., Hocking, D. & Anderson, B. Package ‘rnoaa’ (2022). 2417  
38  
39 [66] Beguería, S. & Vicente-Serrano, S. M. Spei: calculation of the standardised 2418  
40 precipitation-evapotranspiration index. *R package version* **1** (2013). 2419  
41  
42  
43  
44  
45  
46  
47  
48  
49  
50  
51  
52  
53  
54  
55  
56  
57  
58  
59  
60